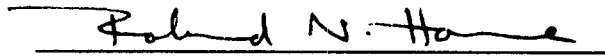


**EFFECTS OF HIGH PRESSURE GRADIENTS ON THE FLOW  
OF  
REAL GASES THROUGH POROUS MEDIA**

A DISSERTATION  
SUBMITTED TO THE DEPARTMENT OF PETROLEUM ENGINEERING  
AND THE COMMITTEE ON GRADUATE STUDIES  
OF STANFORD UNIVERSITY  
IN PARTIAL FULFILLMENT OF THE REQUIREMENTS  
FOR THE DEGREE OF  
DOCTOR OF PHILOSOPHY

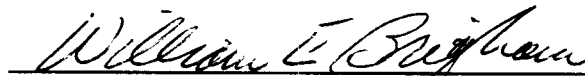
By  
Kwaku Ofori Temeng;  
August 1988

I certify that I have read this thesis and that in my opinion it is fully adequate, in scope and in quality, as a dissertation for the degree of Doctor of Philosophy.



Roland N. Horne  
(Principal Adviser)

I certify that I have read this thesis and that in my opinion it is fully adequate, in scope and in quality, as a dissertation for the degree of Doctor of Philosophy.



William E. Brigham

I certify that I have read this thesis and that in my opinion it is fully adequate, in scope and in quality, as a dissertation for the degree of Doctor of Philosophy.



Henry J. Ramey Jr.

Approved for the University Committee on Graduate Studies:

---

Dean of Graduate Studies

To my wife  
Alice

To our children  
Abena, Tutu, and Aba

## **ACKNOWLEDGEMENTS**

The author wishes to express his sincere appreciation to Dr. Roland N. Horne for his support throughout the course of this work.

Special thanks are also due to Dr. Henry Ramey, Jr., Dr. William Brigham, Dr. Khalid Aziz, and Dr. David Freyberg for serving on the examination committee.

This work was partially supported by Stanford University and the U.S. Department of Energy through the Geothermal Program, Contract Number DE AS07-84ID12529.

## ACKNOWLEDGEMENTS

The author wishes to express his sincere appreciation to Dr. Roland N. Horne for his support throughout the course of this work.

Special thanks are also due to Dr. Henry Ramey, Jr., Dr. William Brigham, Dr. Khalid Aziz, and Dr. David Freyberg for serving on the examination committee.

This work was partially supported by Stanford University and the U.S. Department of Energy through the Geothermal Program, Contract Number DE AS07-84ID12429.

5

# **EFFECTS OF HIGH PRESSURE GRADIENTS ON THE FLOW OF REAL GASES THROUGH POROUS MEDIA**

Kwaku Ofori Temeng, Ph.D.  
Stanford University, 1988.

The flow of gases through homogenous porous media is governed by non-linear differential equations. For steady-state flow the equations may be linearized by assuming small changes in pressure, and thus in fluid properties. The results thus yield a linear relationship between pressure drop and flow rate.

At high flow rates experiments and well tests show deviations from behavior predicted by the linear theory. These deviations are usually attributed to turbulence, inertial effects and other factors, all of which are thought to render Darcy's law invalid. Quadratic and higher order equations are then used to characterize this type of flow, with the nonlinear coefficients determined empirically. However, this study has found that an alternative to using empirically determined non-Darcy effects is to account for the consequences of the assumptions used to linearize the flow equations.

In this study the flow of real gases through porous media was analyzed by incorporating some of the nonlinearities present in the flow equations. It is shown that deviations from linearity of the form observed in field tests and in laboratory experiments can result from the nonlinearities inherent in the basic formulation. Thus, a lack of proportionality between pressure drop and flow rate does not necessarily imply or indicate a deviation from Darcy flow.

In laboratory examples it has been possible to determine observed Forchheimer coefficients, based on a derivation from first principles. This is achieved only with Darcy's law, without reference to non-Darcy effects.

## ACKNOWLEDGEMENTS

The author wishes to express his sincere appreciation to Dr. Roland N. Horne for his support throughout the course of this work.

Special thanks are also due to Dr. Henry Ramey, Jr., ~~Dr.~~ William Brigham, Dr. Khalid Aziz, and Dr. David Freyberg for serving on the examination committee.

This **work** was partially supported by Stanford University and the U.S. Department of Energy through the Geothermal Program, Contract Number DE AS07-84ID12529.

## TABLE OF CONTENTS

1.	Introduction	1
2.	Flow Equations	15
2.1	Basis of Equations	15
2.2	Equation in Terms of Pressure	17
2.3	Equation in Terms of Squares of Pressure	20
2.4	Pseudo Pressure Formulation	25
3.	Rectilinear Flow	26
3.1	Flow Equations	26
3.2	Steady Flow	29
3.2.1	Relationship Between Pressure Drop and Flow Rate	30
3.2.2	Steady-State Pressure Profile	51
3.3	Transient Flow	56
4.	Steady Radial Flow	69
4.1	Formulation	70
4.2	Solution to Steady-State Problem	76
4.3	Simulation of High Rate Gas Wells	82
5.	Stabilized Flow	89
5.1	Formulation	90
5.2	Solution of Stabilized Flow Problem	93
6.	Transient Radial Flow	102
6.1	Drawdown	103
6.2	Injection	113
7.	Conclusions	118
	Nomenclature	121
	References	124

## LIST OF FIGURES

Fig. 1.1	Nonlinear flow of gas through sand	5
Fig. 1.2	Friction factor plot	8
Fig. 2.1	Comparison of $c_g$ and $(c_g - c_\mu)$	19
Fig. 2.2	Correlation of $\mu z$ ( $\gamma_g = 0.6, T = 200^\circ\text{F}$ )	21
Fig. 2.3	Correlation of $\mu z$ ( $\gamma_g = 0.7, T = 175^\circ\text{F}$ )	
Fig. 2.4	Correlation of 'b' parameter	
Fig. 3.1	Comparison of exact and approximate solutions	37
Fig. 3.2	Experimental data of Green and Duwez	39
Fig. 3.3	Flow Behavior of Sample 1 of Cornell (1952)	42
Fig. 3.4	Flow Behavior of Sample 2 of Cornell (1952)	43
Fig. 3.5	Flow Behavior of Sample 3 of Cornell (1952)	44
Fig. 3.6	Flow Behavior of Sample 15 of Cornell (1952)	45
Fig. 3.7	Flow Behavior of Sample 16 of Cornell (1952)	46
Fig. 3.8	Turbulence plots for Samples 15 and 16	48
Fig. 3.9	Flow Behavior of Sample 15 ( $k=500$ md)	49
Fig. 3.10	Flow Behavior of Sample 16 ( $k=600$ md)	50
Fig. 3.11	Steady-state pressure profiles	55
Fig. 3.12	Transient pressure profiles for $t_D = 0.01$	63
Fig. 3.13	Transient pressure profiles for $t_D = 0.05$	64
Fig. 3.14	Transient pressure profiles for $t_D = 0.1$	65
Fig. 3.15	Transient pressure profiles for $t_D = 0.3$	66
Fig. 3.16	Transient pressure profiles for $t_D = 0.4$	67
Fig. 3.17	Transient pressure profiles for $t_D = 0.5$	68
Fig. 4.1	Correlation of 'b' parameter	72
Fig. 6.1	Drawdown pressure behavior	111
Fig. 6.2	Injection pressure behavior	117

## LIST OF TABLES

Table 3.1	Data of Green and Duwez (1951)	40
-----------	--------------------------------	----



# Chapter 1

## Introduction

A fundamental basis for the analysis of flow of fluids through porous media is Darcy's law. Darcy (1856) studied the flow of water through sands under relatively low flow rate conditions. He found that the flow rate was proportional to the pressure gradient, and proposed an equation, which for linear, horizontal flow, is of the form:

$$v = \frac{q}{A} = K \frac{\Delta p}{L} \quad (1.1)$$

where  $v$  is the apparent fluid velocity, and  $K$  is the so-called hydraulic conductivity, an average property of the rock-fluid system.

Experiments conducted with different fluids, and with porous media of different conductivities [Wyckoff et al. (1934), for example], led to an

expression for the conductivity,  $K$ , as the ratio of a property of the rock to that of the fluid, as follows:

$$z = \frac{k \Delta p}{\mu L} \quad (1.2)$$

In **Eq. 1.2**,  $k$  is identified with the permeability of the rock, and is considered independent of the fluid, if the fluid does not react with the porous medium. The property,  $\mu$ , is the Newtonian viscosity of the fluid.

By considering the situation where  $L$  tends to zero in the limit, a more general form of **Eq. 1.2** is obtained as follows:

$$v = \frac{q}{A} = -\frac{k}{\mu} \frac{dp}{dx} \quad (1.3)$$

The negative sign in **Eq. 1.3** is a recognition of the fact that flow is positive in the direction opposite to the pressure gradient. The development of **Eq. 1.3** implies that the properties,  $k$  and  $\mu$ , are in theory, functions of position, and are thus local values. Thus, Darcy's law may be applied to situations involving varying fluid and rock properties.

Hubbert (1956) discussed the implications and application of Darcy's law and defined a flow potential function to account, for the effect of gravity. Hubbert (1956) also derived Darcy's law from fundamental considerations

by using the Navier-Stokes equation.

Darcy's law for the isothermal flow of gas may be derived by integration of Eq. 1.3, and by invoking a gas law equation of state. This gives [Craft and Hawkins (1959)]:

$$\frac{q_{sc}}{A} = \frac{kT_{sc}\Delta p^2}{2\mu L T z p_{sc}} \quad (1.4)$$

where  $q_{sc}$  is the volume flow rate measured at the pressure,  $p_{sc}$ , and temperature,  $T_{sc}$ .

Eq. 1.3 may be combined with the equation of continuity and an appropriate equation of state to derive differential equations for other specific fluids and flow geometries. In general, these differential equations are nonlinear. By assuming small, steady flow rates and constant fluid properties, these equations can be linearized, and can be solved to yield a linear relationship between pressure drop and flow rate.

Muskat (1937) has shown that if the differential equations are expressed in terms of fluid density instead of pressure, then exact linear differential equations are obtained for steady flow. This suggests that for steady flow, analysis may be performed in terms of fluid densities without concern for the consequences of gradient-squared terms as long as Darcy's law applies.

During experimentation involving the flow of water through linear porous systems, Forchheimer (1901) observed that Darcy's law, in the form of Eq. 1.2, did not match high rate data. He proposed a quadratic equation to account for the apparent deviation from Darcy's law, as follows:

$$-\frac{\Delta p}{L} = av + bv^2 \quad (1.5)$$

Forchheimer (1901) pointed out that at even higher rates, third and fourth order terms in  $v$  may be required to match the observed pressure drops.

An apparent deviation from Darcy flow has also been observed during the flow of gases at high rates in linear systems. It has been found [Green and Duwez (1951); Cornell (1952); Cornell and Katz (1953)] that at high gas flow rates, Eq. 1.4 fails to predict pressure drops correctly. The deviation from linearity is illustrated in Fig. 1.1, where flow rate is graphed as a function of the pressure drop [Katz *et al.* (1959)]. The graph shows a deviation from linearity at high flow rate, apparently indicating non-Darcy flow. The result of the apparent non-Darcy effect is a flow rate that is lower than would be expected from pure Darcy flow. Thus, permeability measurements in this flow regime would predict lower than actual values.

The Forchheimer equation has been adapted to model high rate gas flow. This equation is analogous to Eq. 1.5, and is expressed as:

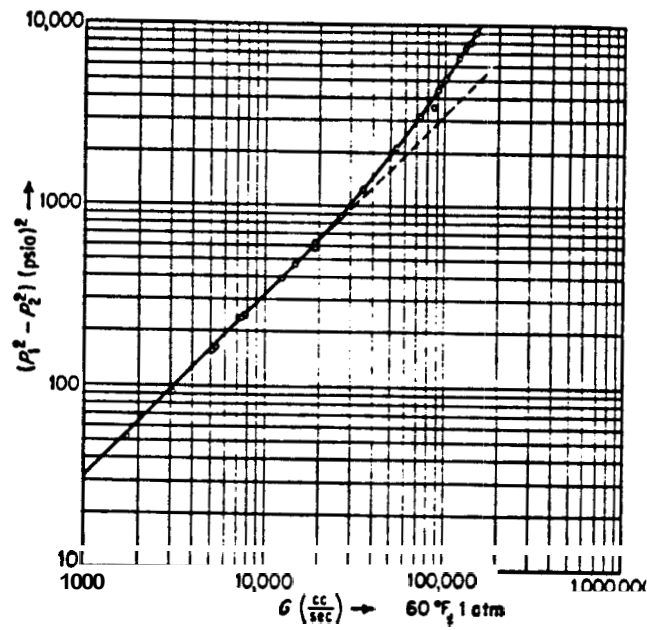


Fig. 1.1 Nonlinear Flow of Air Through Sand  
 [Katz et al. (1959)]

$$-\frac{\Delta p^2}{L} = cq_{sc} + dq_{sc}^2 \quad (1.6)$$

Green and Duwez (1951) employed dimensional analysis to derive a differential form of Forchheimer's equation from first principles, which may be expressed as:

$$-\frac{\partial p}{\partial x} = \frac{\mu}{k}v + \beta\rho v^2 \quad (1.7)$$

where  $\rho$  is the density of the fluid, and  $\beta$  is a property of the porous medium. The term  $\beta$  is usually referred to as a turbulence or inertial factor, or velocity coefficient [Firoozabadi and Katz (1979)].

For application to laboratory core analysis, **Eq. 1.7** may be integrated and combined with the real gas law to give [Cornell (1952)]:

$$\frac{T_{sc}A(p_1^2 - p_2^2)}{2zTL\mu p_{sc}q_{sc}} = \frac{\beta}{\mu} \left( \frac{p_{sc}M}{T_{sc}RA} \right) q_{sc} + \frac{1}{k} \quad (1.8)$$

Thus, a plot of the left hand side of **Eq. 1.8** against  $q_{sc}$  would be linear, with the slope providing a measure of the coefficient,  $\beta$ , and the intercept equal to the reciprocal of permeability.

The cause of the apparent deviation from Darcy flow has been the subject of

a great amount of work and discussion. Because Fancher and Lewis (1933) successfully correlated pressure drop data by means of friction factors and Reynolds number, the deviation from Darcy's law was initially thought to be due to turbulent flow, in analogy with flow through pipes. Firoozabadi and Katz (1979) have summarized discussions on the causes of the non-Darcy flow, and have proposed the use of the term 'velocity coefficient' to describe  $\beta$ .

The velocity coefficient,  $\beta$ , has been widely correlated with rock properties such as porosity and permeability. Katz *et al.* (1959), Tek *et al.* (1962), Gewers and Nichol (1969), Geerstma (1979), Noman *et al.* (1985), Noman and Archer (1987), and Jones (1987) have reported correlations of  $\beta$  with rock properties. Friction factor plots for the characterization of non-Darcy flow have been developed by Fancher and Lewis (1933), Green and Duwez (1951), Cornell and Katz (1953), and others. The friction factor plot of Cornell and Katz (1953) is shown in Fig. 1.2.

The effect of core length on  $\beta$  appears to have been ignored in all the analyses. The importance of the relationship between  $\beta$  and  $L$  is that the transition from the original Forchheimer equation to the differential form requires  $\beta$  and  $L$  to be independent of each other. This is because if  $\beta$  is proportional to  $L$ , for example, then in the limit as  $L$  tends to zero, we obtain Darcy's law (Eq. 1.3), and not the differential Forchheimer equation.

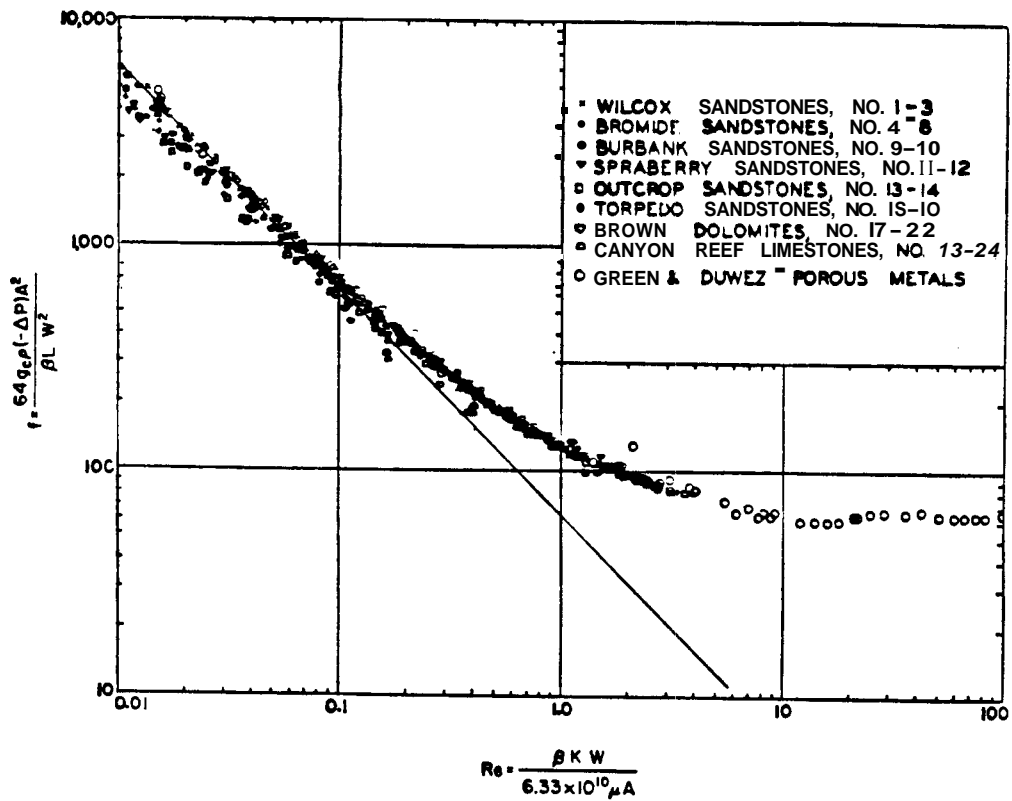


Fig. 1.2 Friction Factor Plot [Cornell and Katz (1953)]

At very high rates, Forchheimer's quadratic equation does not fully describe flow, and a third or fourth power term is required. Ezeudembah and Dranchuk (1982) discussed this high rate flow regime, and derived a cubic equation form of Forchheimer's equation from first principles.

Another type of nonlinear gas flow is slip flow or the Klinkenberg effect. This effect is important in flows at low pressures and through low permeability media, and results in higher than actual calculated permeabilities. Klinkenberg (1941) theorized that the effect arises from the slippage of gas molecules along the rock grain surfaces, and proposed an equation to correct the gas permeability values affected by slip flow. The Klinkenberg effect is not considered in this study. The only effects studied are those related to high velocity flow. The combined effects of gas slippage and 'non-Darcy' flow have been studied by Dranchuk and Piplapure (1973).

Darcy's law may be applied to radial geometries by expressing Eq. 1.3 in terms of radial distance,  $r$ , instead of linear distance,  $x$ . This gives:

$$v = \frac{q}{A} = -\frac{k}{\mu} \frac{dp}{dr} \quad (1.9)$$

For steady flow, Eq. 1.9 may be integrated and combined with the real gas law to produce:

$$q_{sc} = \frac{\pi T_{sc} k h (p_e^2 - p_w^2)}{p_{sc} T \mu z \ln(r_e/r_w)} \quad (1.10)$$

It has been observed that at high flow rates, wells do not produce in accordance with Eq. 1.10., and that a deliverability plot ( $\Delta p^2$  vs  $q_{sc}$ ) on a log-log graph is usually of non-unit slope, suggesting a deviation from Darcy flow. Rawlins and Schellhardt (1936) proposed an empirical equation to account for the apparent deviation from Darcy flow. **This** equation is the famous backpressure equation, and is given **as**:

$$q_{sc} = C(p_e^2 - p_w^2)^n \quad (1.11)$$

where  $C$  and  $n$  are empirically determined constants. It has been shown [Craft and Hawkins (1959)] that  $C$  and  $n$  are not really constants at all, and that  $n$  varies from unity at low flow rates to 0.5 at high flow rates.

Elenbaas and Katz (1948) proposed a formula for computing high velocity flow effects through the use of the friction factor concept.

Another method to empirically consider apparent non-Darcy flow is to express the deliverability equation as a Forchheimer-type equation:

$$\Delta p^2 = a q_{sc} + b q_{sc}^2 \quad (1.12)$$

This method is believed to possess a more fundamental basis than the backpressure equation of **Eq. 1.11** [ERCB (1975); Lee (1982); Ikoku (1984)].

The apparent non-Darcy flow in gas wells has also been interpreted in terms of a rate-dependent skin factor. This is because most of the excess pressure drop due to high velocity flow is thought to occur in the immediate region of the well. Thus for steady-state flow, the pressure drop can be expressed in field units in the form:

$$p_e^2 - p_w^2 = \frac{1.422(10^6)\mu z T q_{sc}}{kh} \left( \ln \frac{r_e}{r_w} + s + Dq \right) \quad (1.13)$$

The ‘non-Darcy’ factor,  $D$ , is usually determined from field tests or approximated from correlations.

In a recent paper, Brigham (1988) showed that the backpressure equation (**Eq. 1.11**) can be related to the Forchheimer equation for stabilized flow to yield estimates of reservoir properties.

Swift and Kiel (1962), and Tek *et al.* (1962) determined the  $D$  coefficient in **Eq. 1.13** analytically by integrating the differential Forchheimer equation for steady, radial flow. The equation derived by Tek *et al.* (1962) is:

$$D = \frac{3.161(10^{-12})\beta\gamma_g z T}{h^2 r_w} \quad (1.14)$$

Noman *et al.* (1985) used this radial Forchheimer equation on North Sea gas wells to calculate and correlate the velocity coefficient,  $\beta$ . Ezeudembah and Dranchuk (1982) developed a similar equation on the basis of a cubic Forchheimer equation.

Rowan and Clegg (1964), in reviewing the work of Houpeurt (1959), concluded that equations of the form given by Eqs. 1.11 and 1.12, do not necessarily indicate non-Darcy flow, and may result from a variation of fluid properties with pressure. This conclusion is not unreasonable because flow through porous media is controlled not just by Darcy's law, but must also conform to material balance requirements. This means that deviation from linearity could arise from a combination of effects, non-Darcy flow possibly being one of them.

Ramey (1965) proposed a method for accounting for non-Darcy flow during unsteady radial flow that incorporated the non-Darcy coefficient,  $D$ . Tek *et al.* (1962) used finite difference methods to study unsteady, non-Darcy flow. Wattenbarger and Ramey (1968) studied the composite effects of high flow velocity, wellbore storage, and skin effect on unsteady real gas flow.

Non-Darcy effects during unsteady real gas flow is usually described in terms of a Forchheimer-type equation, but with a time-independent non-Darcy coefficient [Lee 1982]. Lee *et al.* (1987) combined the differential Forchheimer equation with the continuity equation to develop a general

differential equation for high velocity flow. They concluded that the coefficient,  $D$ , is in general pressure-dependent, and that at high flow rates, significant errors are introduced by assuming a constant  $D$  factor.

The partial differential equation for Darcy flow of real gas is obtained by combining the differential form of Darcy's law with the equation of continuity. The result, in terms of pressure or pressure-squared, is a nonlinear partial differential equation that does not possess general solutions. A similar equation results from the analysis of liquid flow. Finjord and Aadnoy (1986), Finjord (1987), and Odeh and Babu (1987) have studied some of the nonlinearities present in the liquid equation. Al-Hussainy and Ramey (1966) discussed the use of the gas pseudo-pressure,  $m(p)$ , and showed that it eliminates the gradient-squared nonlinearity in the real gas partial differential equation. Russel *et al.* (1966) also discussed the use of a similar pseudo-pressure to simplify the real gas partial differential equation.

The  $m(p)$  function has become the standard variable for the analyses of gas well tests [ERCB (1975)]. However, certain conclusions drawn from earlier analyses, using squares of pressure, have been carried over to the  $m(p)$  analyses without due consideration for the consequences. For example, non-Darcy flow is considered in the  $m(p)$  formulation by including a non-Darcy  $D$  term, by analogy with the pressure-squared formulation [ERCB (1975)].

In this work, the effects of the gradient-squared nonlinearity in the real gas flow equation are studied. The scope of the study includes steady and unsteady rectilinear flow through cores, and radial, steady, pseudo-steady and transient flow. The relationship between pressure drop and flow rate are determined, and related back to apparent non-Darcy flow.

# Chapter 2

## Flow Equations

In this chapter are presented the equations and assumptions used to formulate the problems considered in this study. Equations are discussed in terms of pressure, pressure-squared, and pseudo-pressure. Methods are also discussed for estimating the coefficients of some of the terms in the equations. The equations discussed here are all derived in Al-Hussainy (1967) and ERCB (1975). We discuss the final forms that will be used in subsequent analyses.

### 2.1 Basis for Equations

The derivations of the differential equations all assume that Darcy's law is valid, and that the real gas law applies. By combining the equation of continuity with Darcy's law and an equation of state, these result in

nonlinear differential equations that are presented in the following. These three principles are expressed in the following.

**Darcy's Law for Horizontal Flow:**

$$\vec{v} = -\frac{k}{\mu} \nabla p \quad (2.1)$$

**Continuity Equation:**

$$\nabla \cdot (\rho \vec{v}) = -\frac{\partial}{\partial t} (\rho \phi) \quad (2.2)$$

**Equation of State:**

$$\rho = \frac{pM}{zRT} \quad (2.3)$$

In addition to the preceding equations, the following assumptions **are** also made:

- o Isothermal Flow
- o Constant porosity,  $\phi$
- o Constant and isotropic permeability,  $k$

Using these equations and assumptions, differential equations can be developed in terms of pressure, pressure-squared or pseudo-pressure variables. In this study, the pressure formulation has been used to study the flow of gas through cores, and radial gas flow studies were performed on the basis of a pressure-squared differential equation. An equation in terms of pseudo-pressure is presented for purposes of comparison and discussion.

## 2.2 Equation in Terms of Pressure

In terms of pressure, the partial differential equation of real gas flow in porous media is:

$$\nabla^2 p - \frac{d}{dp} \left[ \ln \left( \frac{\mu z}{p} \right) \right] (\nabla p)^2 = \frac{\phi \mu c}{k} \frac{\partial p}{\partial t} \quad (2.4)$$

Eq. 2.4 is nonlinear because of the presence of the squared-gradient term, and because the coefficient of the time derivative term is in general, pressure-dependent.

The coefficient of the squared-gradient term in Eq. 2.4 may be expressed in the following alternative form:

$$\frac{d}{dp} \left[ \ln \left( \frac{\mu z}{p} \right) \right] = \frac{p}{\mu z} \left[ \frac{1}{p} \frac{d(\mu z)}{dp} - \frac{\mu z}{p^2} \right]$$

$$\begin{aligned}
&= \frac{1}{\mu z} \frac{d(\mu z)}{dp} - \frac{1}{p} \\
&= \frac{1}{z} \frac{dz}{dp} + \frac{1}{\mu} \frac{d\mu}{dp} - \frac{1}{p}
\end{aligned} \tag{2.5}$$

**Eq. 2.4** then becomes:

$$\nabla^2 p + (c_g - c_\mu)(\nabla p)^2 = \frac{\phi \mu c}{k} \frac{\partial p}{\partial t} \tag{2.6}$$

where:

$$c_g = \frac{1}{p} - \frac{1}{z} \frac{dz}{dp} \tag{2.7}$$

is the isothermal gas compressibility, and where:

$$c_\mu = \frac{1}{\mu} \frac{d\mu}{dp} \tag{2.8}$$

For most of the range of pressure values that are of interest, the isothermal gas compressibility is the dominant variable of the two coefficient terms. This is demonstrated in Fig. 2.1 which shows a comparison  $(c_g - c_\mu)$  and  $c_g$  for a gas of  $\gamma_g = 0.7$  and a temperature of  $75^\circ F$  for a range of pressures. For most pressure ranges, the error introduced by using only the

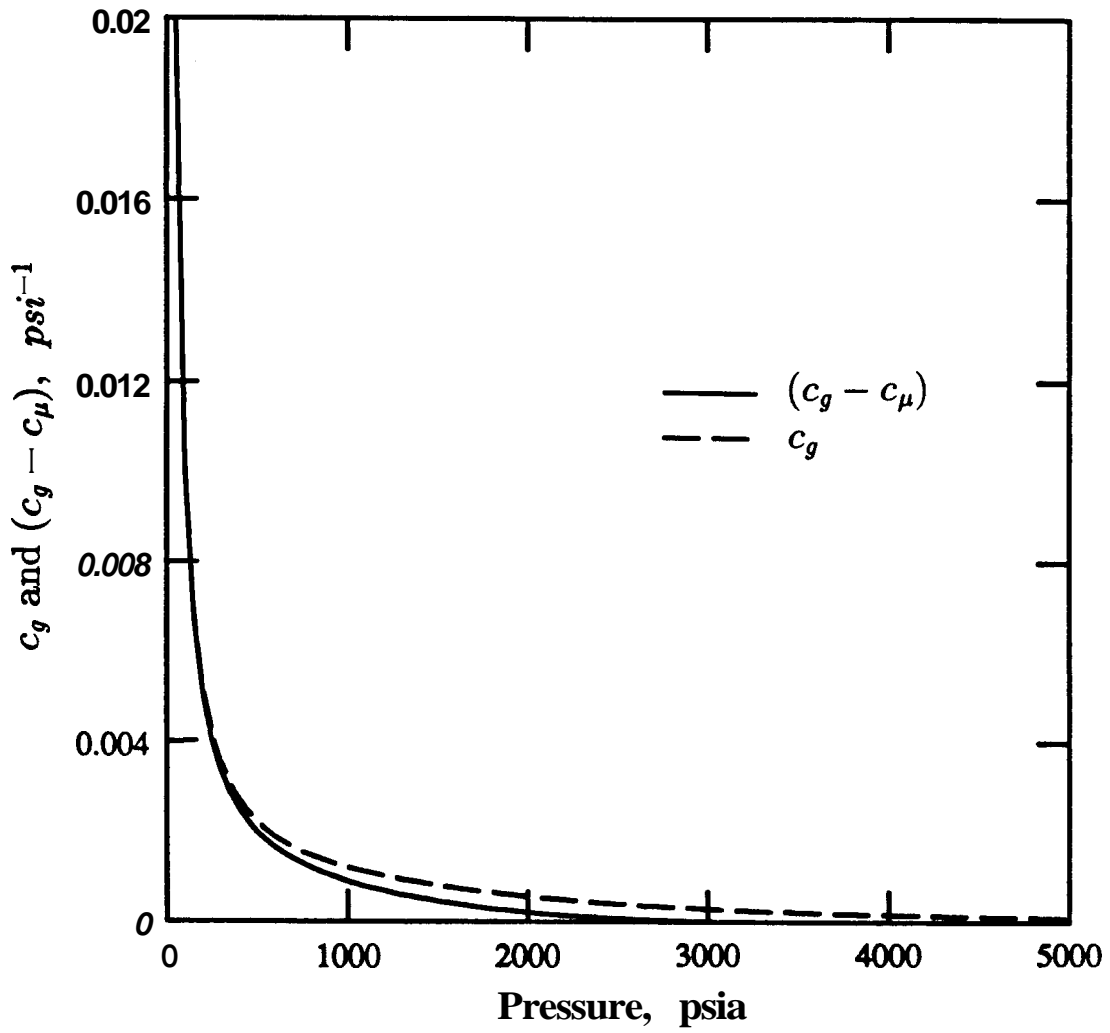


Fig. 2.1 Comparison of  $c_g$  and  $(c_g - c_\mu)$

gas compressibility as the coefficient of the squared gradient term will be reasonably small.

Fig. 2.1 shows that for high values of pressure, the coefficient,  $(c_g - c_\mu)$  is very nearly zero. This practically removes the effect of the squared-gradient term in the differential equation. This observation is consistent with that of Aziz *et al.* (1976), who arrived at the same conclusion using a different method of interpretation.

### 2..3 Equations in Terms of Squares of Pressure

The flow equation in terms of squared-pressure is given by:

$$\nabla^2 p^2 - \frac{d}{dp^2} [\ln(\mu z)] (\nabla p^2)^2 = \frac{\phi \mu c}{k} \frac{\partial p^2}{\partial t} \quad (2.9)$$

The coefficient of the nonlinear gradient-squared term may be expressed in a slightly different way as follows:

$$\frac{d}{dp^2} [\ln(\mu z)] = \frac{1}{\mu z} \frac{d(\mu z)}{dp^2} \quad (2.10)$$

Figs. 2.2 and 2.3 show behavior of  $\mu z$  with pressure for gases of different properties. The nature of the curves suggests that  $\mu z$  may be correlated according to the equation:

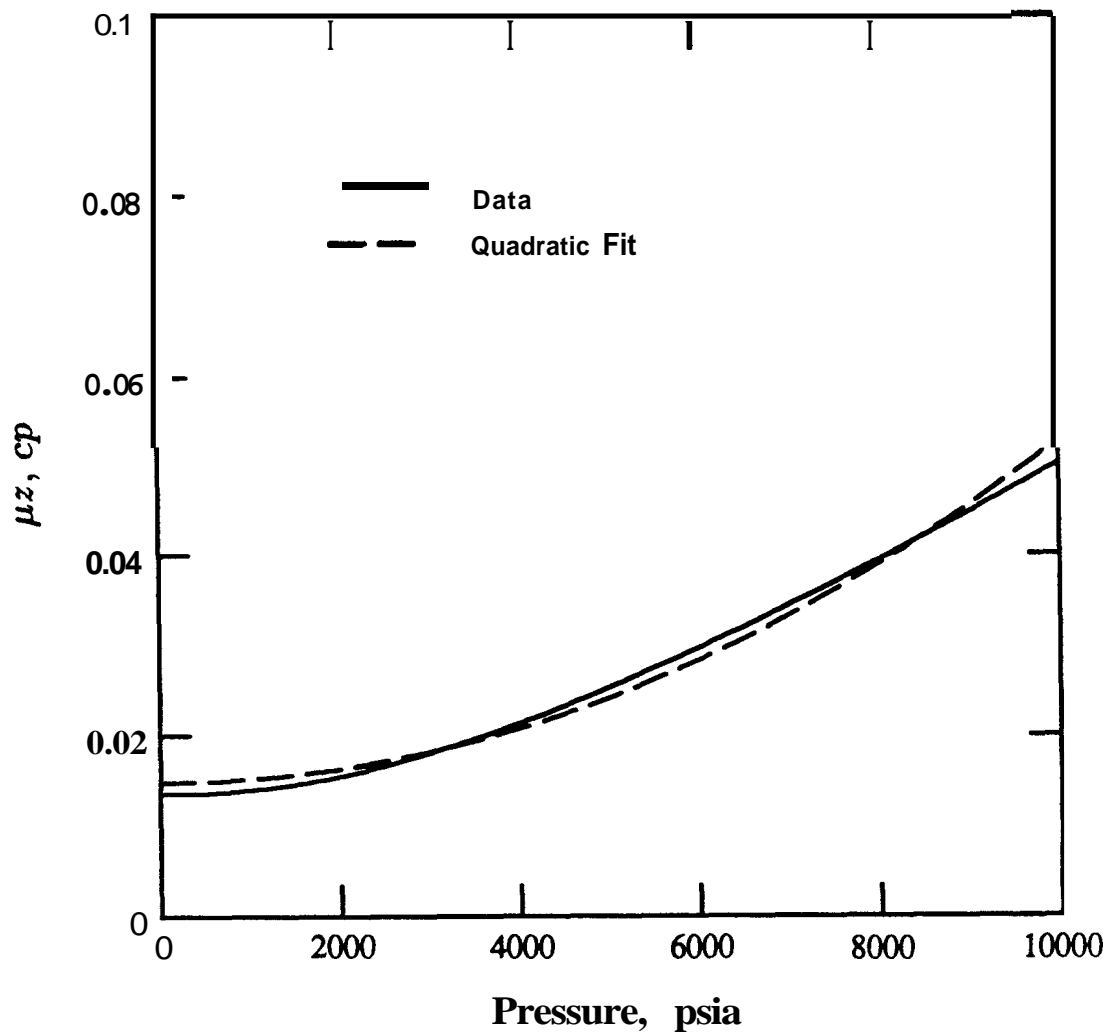


Fig. 2.2 Correlation of  $\mu z$  ( $\gamma_g = 0.6$ ,  $T = 200^\circ F$ )

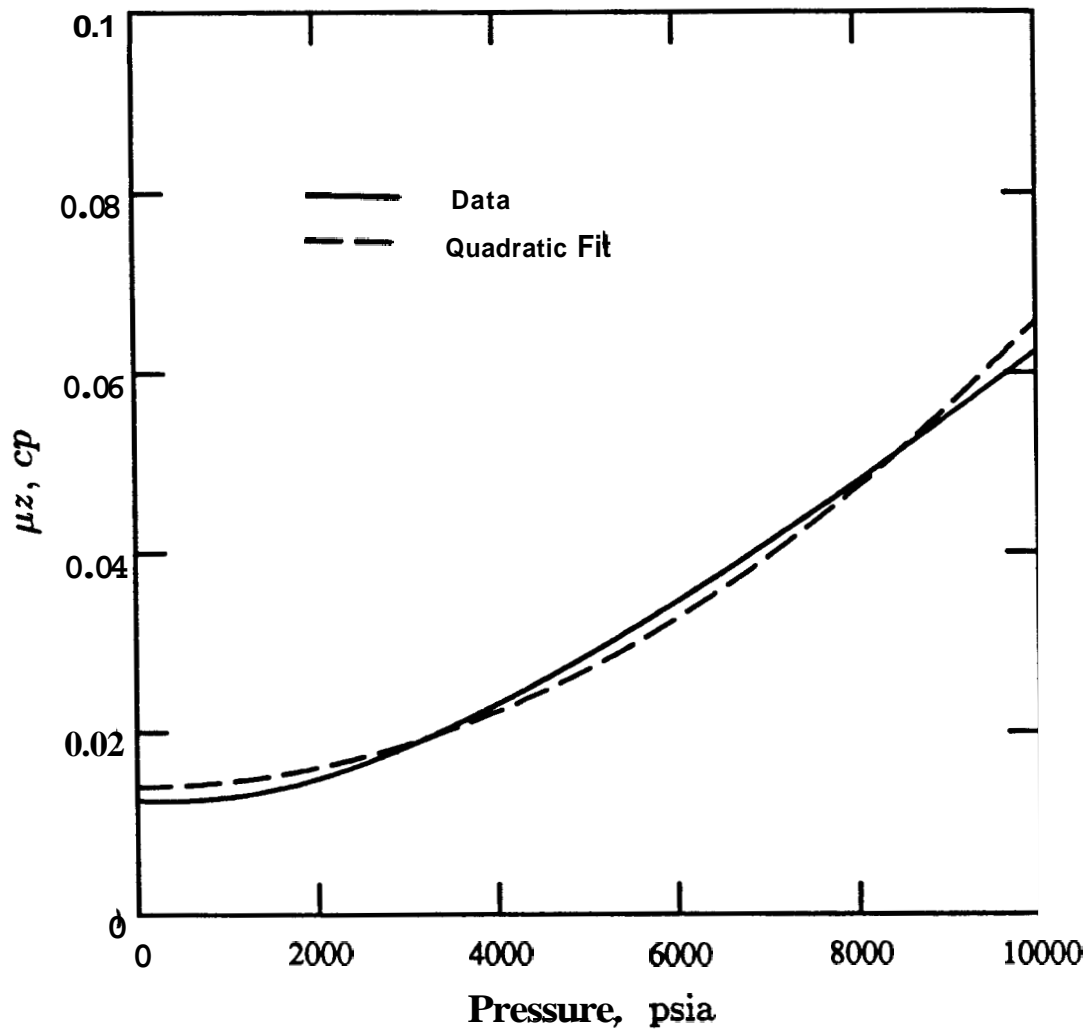


Fig. 2.3 Correlation of  $\mu_z$  ( $\gamma_g = 0.7$ ,  $T = 175^\circ\text{F}$ )

$$\mu z = a + bp^2 \quad (2.11)$$

The correlation was tested for sweet natural gases of different gravities and temperatures, and seem to **work** fairly well. For purposes of developing the correlation, the  $z$  factor was calculated using a correlation developed by Dranchuk *et al.* (1974). Viscosity was calculated by means of the correlation of Lee *et al.* (1966), and the critical temperature and pressure by the equations of Thomas *et al.* (1970).

The dashed lines in Fig 2.2 and 2.3 represent calculations of  $\mu z$  based on Eq. 2.11. At low pressures below about 100 *psia*,  $\mu z$  decreases slightly with pressure, and cannot be described by the same coefficients in Eq. 2.11 as for the higher pressure values. Figure 2.4 presents a correlation of the parameter,  $b$  versus temperature, and shows that  $b$  is large for low temperatures and high specific gas gravities. The parameter  $b$  is of the order of  $10^{-9}$  *cp/psi*<sup>2</sup>.

The flow equation in terms of  $p^2$  may be approximated by:

$$\nabla^2 p^2 - \frac{b}{\mu z} (\nabla p^2)^2 = \frac{\phi \mu c}{k} \frac{\partial p^2}{\partial t} \quad (2.12)$$

The coefficient of the gradient-squared term is pressure-dependent because of the presence of the  $\mu z$  product in the denominator. The coefficient can

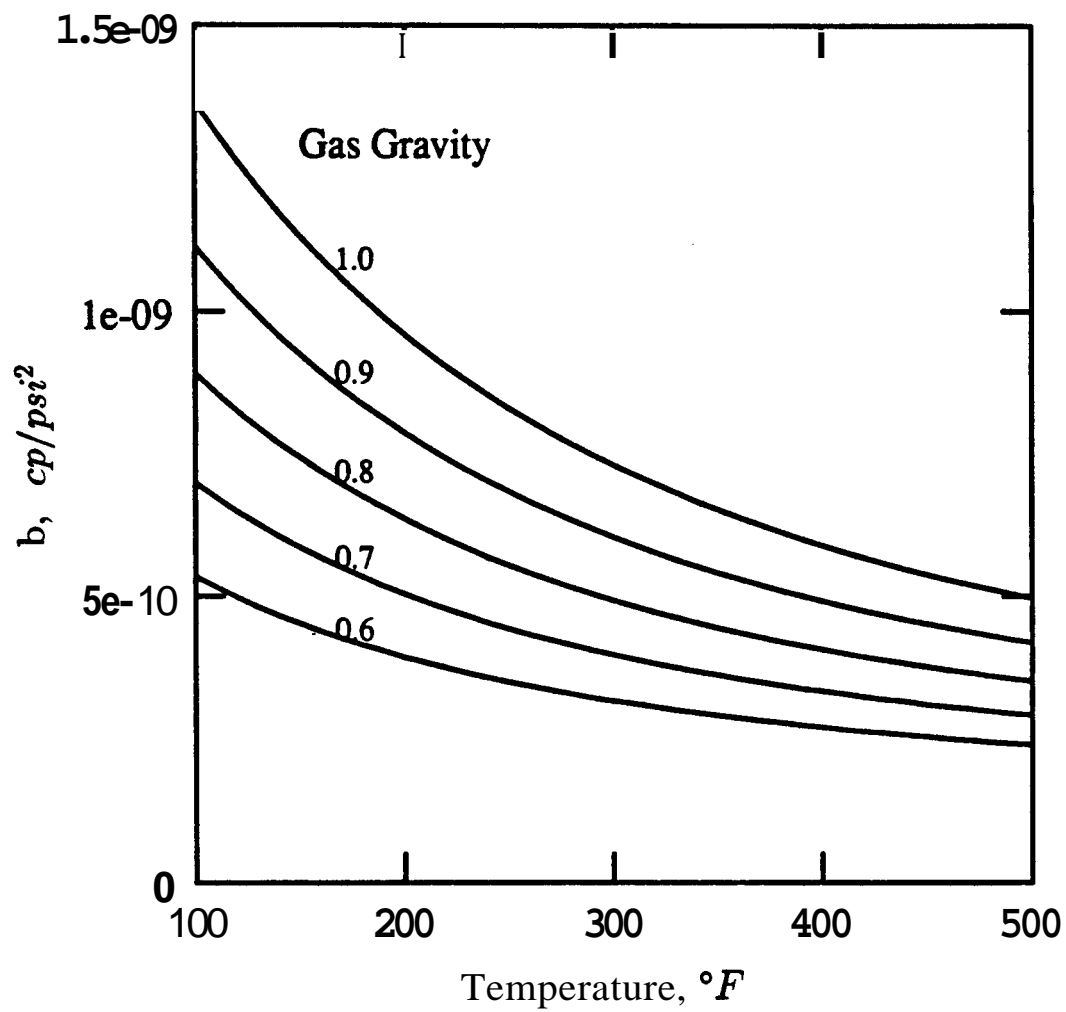


Fig. 2.4 Correlation of 'b' parameter

be made constant by expressing  $\mu z$  at a known average pressure. This is discussed in Chapter 4.

## 2.4 Pseudo-Pressure Formulation

Al-Hussainy *et al.* (1966) introduced the concept of the real gas pseudo-pressure for the analysis of gas flow:

$$m(p) = 2 \int_{p_b}^p \frac{p}{\mu z} dp \quad (2.13)$$

where  $p_b$  is some base pressure.

In terms of  $m(p)$ , the flow equations become:

$$\nabla^2 m = \frac{\phi \mu c}{k} \frac{\partial m}{\partial t} \quad (2.14)$$

The equation in terms of  $m(p)$  is still nonlinear because of the fact that  $\mu$  and  $c$  depend upon  $m$ . However gradient squared terms are incorporated in this substitution.

# Chapter 3

## Rectilinear Flow

This chapter presents an analysis of the real gas flow through a finite, linear porous medium. The objective is to model and study high rate flow in laboratory cores. A relationship between flow rate and pressure drop for steady flow and will be presented. The discussion will include the pressure-distance profiles that result from high rate flow during both steady and unsteady flow. The equations developed will be matched to experimental results that are available in the literature.

### 3.1 Flow Equations

The subject problem is the flow of a real gas in a finite core of length  $L$ , and constant cross-sectional area,  $A$ . The pressures at the upstream and downstream ends of the core are fixed at pressures  $p_1$  and  $p_2$  respectively.

The effects of gas slippage are not included in the analysis.

As discussed in Chapter 2, the partial differential equation governing gas flow is given by Eq. 2.6. When this is expressed for linear flow, it becomes:

$$\frac{\partial^2 p}{\partial x^2} + (c_g - c_\mu) \left( \frac{\partial p}{\partial x} \right)^2 = \frac{\phi \mu c}{k} \left( \frac{\partial p}{\partial t} \right) \quad (3.1)$$

where:

$$c_g = \frac{1}{\rho} \frac{\partial \rho}{\partial p} \Big|_T \quad (3.2)$$

and:

$$c_\mu = \frac{1}{\mu} \frac{\partial \mu}{\partial p} \Big|_T \quad (3.3)$$

The pressure equation was chosen to model gas flow because the range of pressure drops considered in this problem is small. This means that to use either the squared pressure or the pseudo-pressure formulation, very accurate viscosity and  $z$  factor data at small pressure intervals would be required. Such data are not available. The pressure formulation involves primarily the gas compressibility as the coefficient of the squared-gradient term, and is easier to estimate.

In this study, attention has been focused on the effects of the squared-gradient nonlinearity in the differential equation. The coefficient of the squared-gradient term is strongly dependent on pressure, especially at the low pressures used in laboratory experiments that are modeled in this **work**. To make the problem tractable however, an average value of the coefficient will be determined and utilized in the analysis. Because the coefficient of the gradient-squared term is strongly pressure-dependent, no single average value can model the flow over the entire range of pressure drops. However, a good average can be chosen to provide a solution with an order of magnitude accuracy.

The average coefficient used in this study was determined by performing an integration over the length of the core. The integration was performed to produce the following result:

$$\bar{c} = \overline{(c_g - c_\mu)} = \frac{1}{\Delta p} \int_{p_2}^{p_1} \left( -\frac{1}{z} \frac{dz}{dp} + \frac{1}{p} - \frac{1}{\mu} \frac{d\mu}{dp} \right) dp \quad (3.4)$$

$$= \frac{1}{\Delta p} \ln \left( \frac{z_2 p_1 \mu_2}{z_1 p_2 \mu_1} \right) \quad (3.5)$$

where:

$$\Delta p = p_1 - p_2 \quad (3.6)$$

For flows at relatively low pressures, as usually pertain in laboratory experiments, there is little change in viscosity and in the compressibility factor from inlet to outlet. Equation 3.5 then becomes:

$$\bar{c} = \frac{1}{\Delta p} \ln \left( \frac{p_1}{p_2} \right) \quad (3.7)$$

## 3.2 Steady Flow

In steady-state flow there is no dependence of pressure on time, and the mass flow rate of gas at every location is constant. For this situation, the right side of Eq. 3.1 can be equated to zero. The partial differential equation then becomes:

$$\frac{d^2 p}{dx^2} + \bar{c} \left( \frac{dp}{dx} \right)^2 = 0 \quad (3.8)$$

Two different types of analysis will be performed. The first one will relate pressure drop to flow rate, and the second will provide a description of the pressure-length profile in the core. The two problems differ only in the way the boundary conditions are specified.

### 3.2.1 Relationship Between Pressure Drop and Flow Rate

In this section an equation relating pressure drop and flow rate during steady-state flow will be presented. We consider the situation where gas is injected at a constant rate,  $q_{sc}$ , at one end of a core, and produced at the outlet end whose pressure is fixed at  $p_2$ .

The boundary condition at the inlet end is:

$$\frac{\partial p}{\partial x} = -\frac{q_{sc}\mu p_{sc}Tz}{kAp_mT_{sc}}, \quad \text{at } x = 0 \quad (3.9)$$

The outlet condition is:

$$p = p_2, \quad \text{at } x = L \quad (3.10)$$

The following dimensionless variables are introduced:

$$x_D = \frac{x}{L} \quad (3.11)$$

$$p_D = \frac{kAp_mT_{sc}}{q_{sc}L\mu zTp_{sc}} [p(x) - p_2] \quad (3.12)$$

The flow equations then become:

$$\frac{d^2 p_D}{dx_D^2} + \alpha_1 \left( \frac{dp_D}{dx_D} \right)^2 = 0 \quad (3.13)$$

$$p_D = 0, \quad \text{at} \quad x_D = 1 \quad (3.14)$$

$$\frac{dp_D}{dx_D} = -1, \quad \text{at} \quad x_D = 0 \quad (3.15)$$

where:

$$\alpha_1 = \frac{\bar{c}q_{sc}\mu z L p_{sc} T}{k A p_m T_{sc}} \quad (3.16)$$

The parameter,  $\alpha_1$ , can be interpreted as a measure of the significance of the nonlinear squared-gradient term in the differential equation. Thus the nonlinearity is important for high flow rates, high compressibility, low permeability, and low mean pressure.

**Eq. 3.13** may be solved by making the substitution:

$$u = \frac{dp_D}{dx_D} \quad (3.17)$$

to obtain the integrable equation:

$$\frac{du}{dx_D} + \alpha_1 u^2 = 0 \quad (3.18)$$

The inlet boundary condition in  $u$ , corresponding to Eq. 3.15, is:

$$u = -1, \quad \text{at} \quad x_D = 0 \quad (3.19)$$

The solution to Eq. 3.18, subject to the boundary condition of Eq. 3.19 is:

$$u = \frac{1}{\alpha_1 x_D - 1} = \frac{dp_D}{dx_D} \quad (3.20)$$

and can be further integrated, and combined with Eq. 3.14, to obtain the final solution:

$$p_D = \frac{1}{\alpha_1} \ln \left( \frac{1 - \alpha_1 x_D}{1 - \alpha_1} \right) \quad (3.21)$$

The total pressure drop across the core may be obtained by substituting unity for  $x_D$  in Eq. 3.21. This gives:

$$p_{TD} = -\frac{1}{\alpha_1} \ln(1 - \alpha_1) \quad (3.22)$$

The overall, dimensional pressure gradient is therefore given by:

$$\frac{\Delta p}{L} = -\frac{1}{\bar{c}L} \ln \left( 1 - \frac{L\bar{c}q_{sc}\mu z T p_{sc}}{kA p_m T_{sc}} \right) \quad (3.23)$$

The flow rate,  $q_{sc}$ , may be obtained by rearranging Eq. 3.23, and gives:

$$q_{sc} = \frac{kA p_m T_{sc}}{L\bar{c}\mu p_{sc} T z} \left( 1 - e^{-\bar{c}\Delta p} \right) \quad (3.24)$$

To examine the nature of the solution obtained, Eq. 3.22 may be expanded in a Taylor series in terms of  $\alpha_1$  as follows:

$$p_{TD} = 1 + \frac{\alpha_1}{2} + \frac{\alpha_1^2}{3} + \dots \quad (3.25)$$

In terms of the dimensional variables, Eq. 3.25 becomes:

$$\frac{\Delta p}{L} = A_1 q_{sc} + B_1 q_{sc}^2 + C_1 q_{sc}^3 + \dots \quad (3.26)$$

where:

$$A_1 = \left( \frac{\mu z T p_{sc}}{kA p_m T_{sc}} \right) \quad (3.27)$$

$$B_1 = \frac{\bar{c}L}{2} \left( \frac{\mu z T p_{sc}}{k A p_m T_{sc}} \right)^2 = \frac{\bar{c}L}{2} A_1^2 \quad (3.28)$$

$$C_1 = \frac{(\bar{c}L)^2}{3} \left( \frac{\mu z T p_{sc}}{k A p_m T_{sc}} \right)^3 = \frac{(\bar{c}L)^2}{3} A_1^3 \quad (3.29)$$

Equation 3.26 can be expressed in terms of  $\Delta p^2$  by multiplying through by twice the mean pressure. Thus:

$$\frac{\Delta p^2}{L} = 2A_1 p_m q_{sc} + 2B_1 p_m q_{sc}^2 + 2C_1 p_m q_{sc}^3 \quad (3.30)$$

If only the first two terms are retained, Eq. 3.30 can be written as:

$$\frac{\Delta p^2}{L} = \left( \frac{2\mu z T p_{sc}}{k A T_{sc}} \right) q_{sc} + \frac{\bar{c}L}{p_m} \left( \frac{\mu z T p_{sc}}{k A T_{sc}} \right)^2 q_{sc}^2 \quad (3.31)$$

Equations 3.26 and 3.31 indicate a nonlinear relationship between pressure drop and flow rate. They are of the Forchheimer type, which is usually cited as evidence of non-Darcy behavior. As was shown in Chapter 2 however, the basis of the equations are merely Darcy's law and a material balance. This suggests the likelihood that some flows that have been described as non-Darcy may not be so at all, but may be due to the gradient-squared non-linearity of the governing differential equation. The equations also show

that the coefficients of the nonlinear terms are functions not only of compressibility, but also of the length of the core. Thus, if  $L$  is made to go to zero in the limit, we should recapture Darcy's law, and not a differential form of the Forchheimer equation.

The first term in Eq. 3.31 is the linear or so-called Darcy term, which will be referred to here as the 'laminar' term. The additional terms are therefore equivalent to what have been referred to as 'non-Darcy', 'turbulent', or 'inertial' terms.

To relate the results to the non-Darcy parameter,  $\beta$ , Eq. 3.31 may be rearranged to give:

$$\frac{T_{sc}A\Delta p^2}{2\mu zTLp_{sc}q_{sc}} = \frac{1}{k} + \frac{\bar{c}L\mu zTp_{sc}}{2p_m k AT_{sc}} q_{sc} \quad (3.32)$$

Comparison with Eq. 1.8 leads to the following definition for  $\beta$ :

$$\beta = \left( \frac{\bar{c}\mu^2 zTR}{2p_m k^2 MT_{sc}} \right) \quad (3.33)$$

or:

$$\beta = \frac{\bar{c}L\mu^2}{2k^2\rho T_{sc}} \quad (3.34)$$

Figure 3.1 shows a graph of  $p_D$  vs  $\alpha_1$  (Eq. 3.25), and demonstrates that at high values of  $\alpha_1$ , corresponding to high flow rates or low permeabilities, more terms in the expansion equation would be required to describe the flow accurately. The figure also indicates that for flows corresponding to  $\alpha_1 = 1$ , the behavior becomes ‘critical’, i.e. an infinite pressure drop is required to produce an additional increase in flow rate.

Figure 3.1 also suggests guidelines for determining the number of Forchheimer terms required to approximate the exact solution. It shows that ‘laminar’ flow is accurate to a value of  $\alpha_1$  of about **0.05**. The two term Forchheimer equation is valid to a value of  $\alpha_1$  of about **0.3**, whereas the three term equation is good for  $\alpha_1$  less than **0.45**. Thus, determination of  $\alpha_1$  would provide an indication of the number of terms in Forchheimer’s equation required to describe the flow. In any case, since the relationship between pressure drop and flow rate is also given in a simple closed form in Eq. 3.24, it is not necessary in general to resort to the Forchheimer formulation at all.

To show that the deviation from linearity (‘turbulence’) is not due to non-Darcy effects, the equation derived here was matched with experimental data. Two sets of experiments were analyzed; the first set was reported by Green and Duwez (1951), and the second set by Cornell (1952). The description and analyses of these data follow.

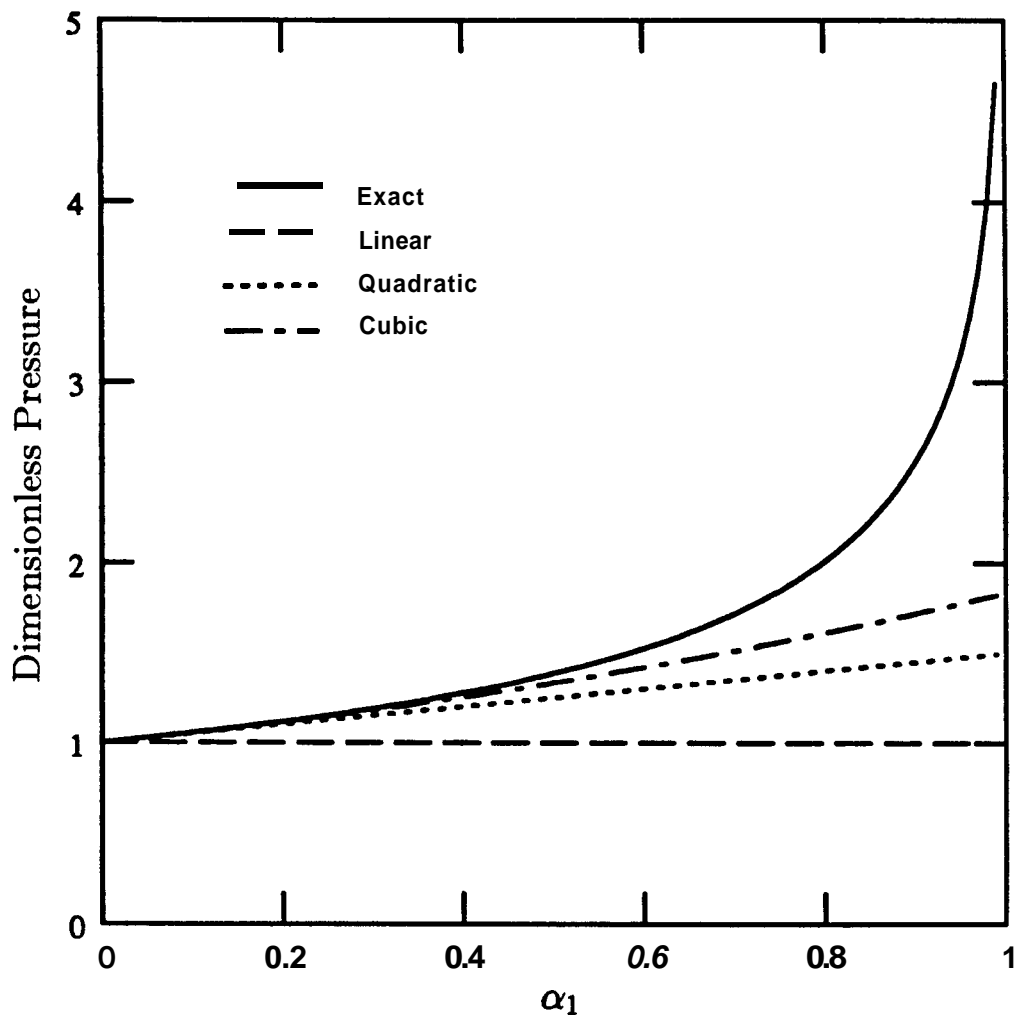


Fig. 3.1 Comparison of Exact and Approximate Solutions

### **Data of Green and Duwez (1951)**

The experiments of Green and Duwez (1951) involved flowing nitrogen gas at various rates through  $\frac{1}{4}$  inch thick porous metals of different permeabilities. The diameter of the metal samples was 1.4 inches. The porosities varied from 0.256 to 0.595, and the permeabilities from **64** millidarcies to 19 Darcies. Figure **3.2** is a plot of their experimental results. The data for the 19-Darcy sample (sample C) were ignored because the reported permeability was estimated, not actually measured. The temperature was not reported, and therefore it was assumed to be  $75^\circ F$  for the purpose of using the equations derived in this work.

To compare the experimental results to the equations derived in the study, a few experimental points were selected from Fig. **3.2**. Because the grid of the graph is coarse, the points were selected to coincide as much as possible with the grid crossings. All the points were chosen from the nonlinear sections of the curves.

Table **3.1** is a summary of the comparison of the experimental flow rate with computed flow rate based on Eq. **3.24**. The agreement between the experimental and computed data is reasonable. The lack of better agreement is probably due to the error involved in averaging the compressibility term in the flow equation over such a large pressure drop.

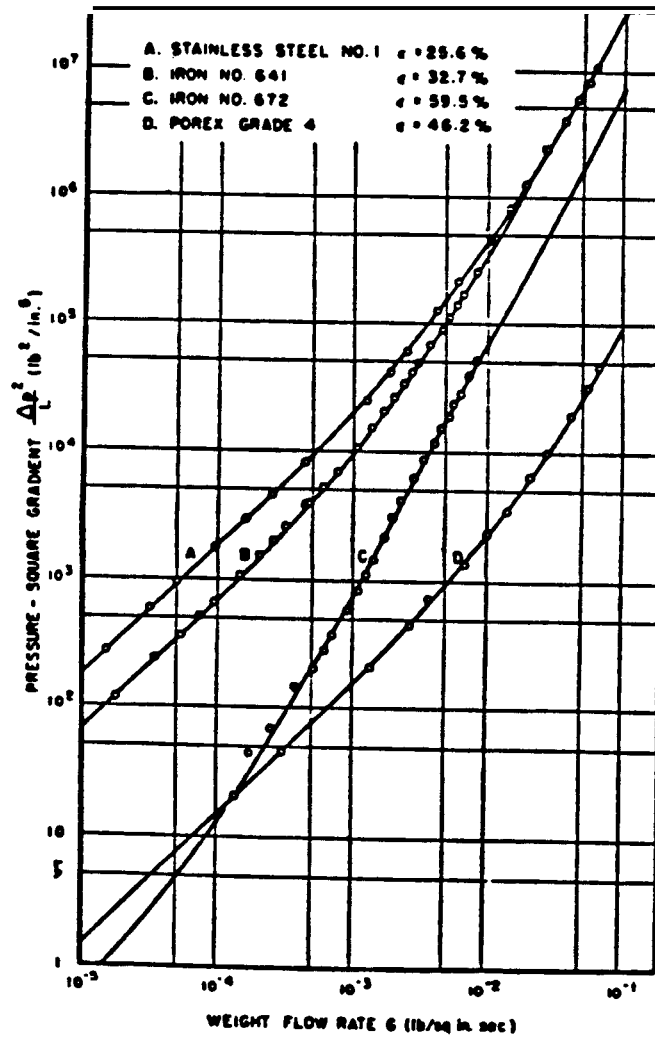


Fig. 3.2 Experimental Data of Green and Duwez (1951)

**TABLE 3.1**

**Data of Green and Duwez (1951)**

Sample	$k$ (md)	$\Delta p^2/L$ ( $lb^2/in^5$ )	$Ap$ (psi)	Measured Rate ( $lb/in^2 - sec$ )	Predicted Rate ( $lb/in^2 - sec$ )
A	63.9	$5(10^5)$	339.2	$10^{-2}$	7.5(
A	63.9	107	1566.5	7(	$10^{-1}$
B	178	104	37.4	$10^{-3}$	$0.9(10^{-3})$
B	178	$5(10^4)$	98.1	$3(10^{-3})$	$3.2(10^{-3})$
B	178	105	144.1	$5(10^{-3})$	$5.1(10^{-3})$
C	7080	104	37.4	$3(10^{-2})$	$3.3(10^{-2})$

### Data of Cornell (1952)

Cornell (1952) performed a series of experiments on rock samples of different permeabilities and sizes. Different gases were flowed at varying rates in order to determine correlations for the nonlinear term,  $\beta$ . The permeability and  $\beta$  both were determined from the same plot through Eq. 1.8 which is:

$$\frac{T_{sc}A(p_1^2 - p_2^2)}{2\mu zTLp_{sc}q_{sc}} = \frac{\beta}{\mu} \left( \frac{p_{sc}M}{T_{sc}RA} \right) q_{sc} + \frac{1}{k} \quad (3.35)$$

The permeability determined for the low-permeability samples using this method appeared to be in error as a result of the Klinkenberg effect. Since the Klinkenberg effect was not considered in deriving the equations in this work, the comparisons were made only with the high permeability data (greater than 100 md). This was in order to avoid the influence of Klinkenberg flow on the results.

Figures 3.3 to 3.7 show graphs of measured and calculated flow rates versus pressure drop. The agreement is in general reasonable given the fact that an average value of a strongly pressure-dependent parameter is used as a coefficient in the equation. In two of the cases (Samples 15 and 16), the model appears to exaggerate the nonlinear effects. This lack of agreement is probably a result of using the wrong values of permeability in the model. The reported permeabilities were obtained from a plot based on Eq. 3.35,

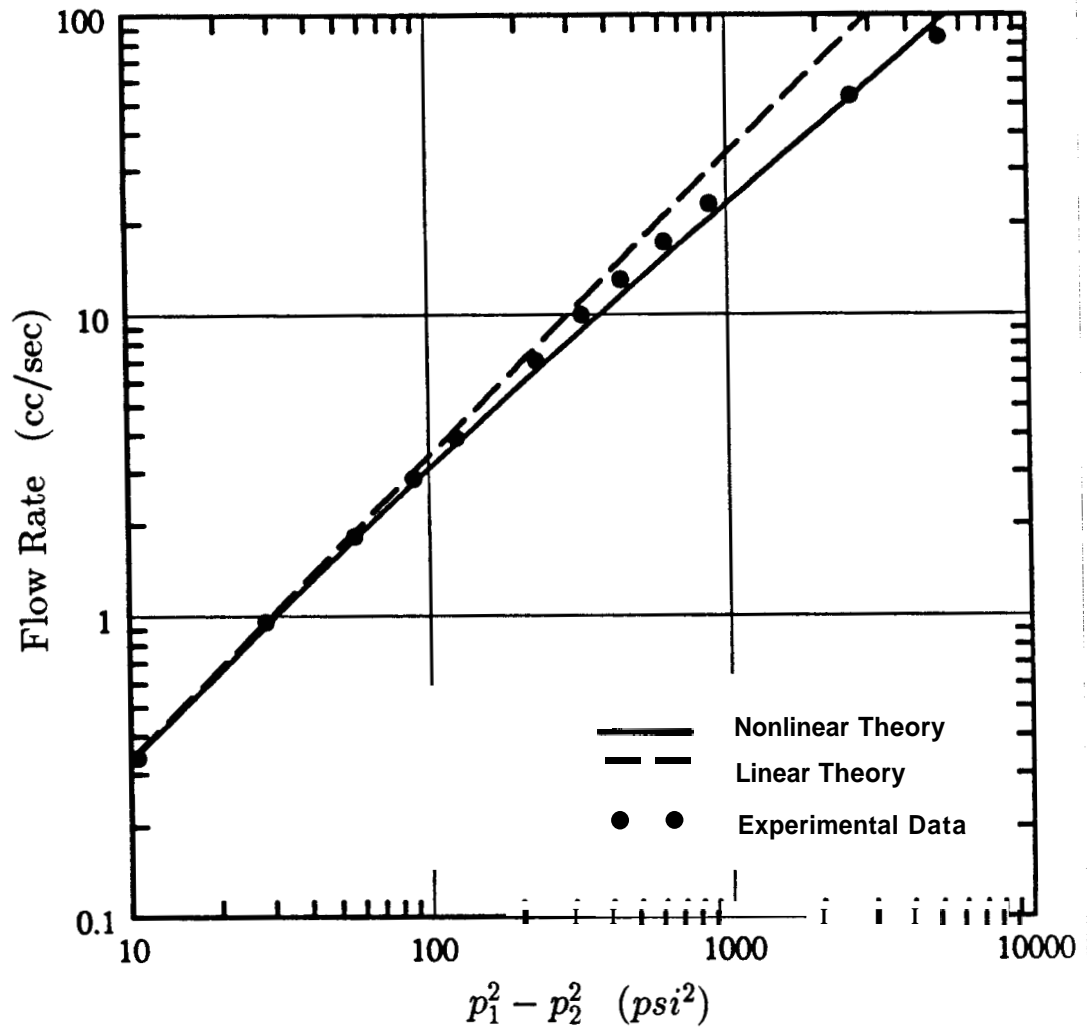


Fig. 3.3 Flow Behavior of Sample 1 of Cornell (1952)

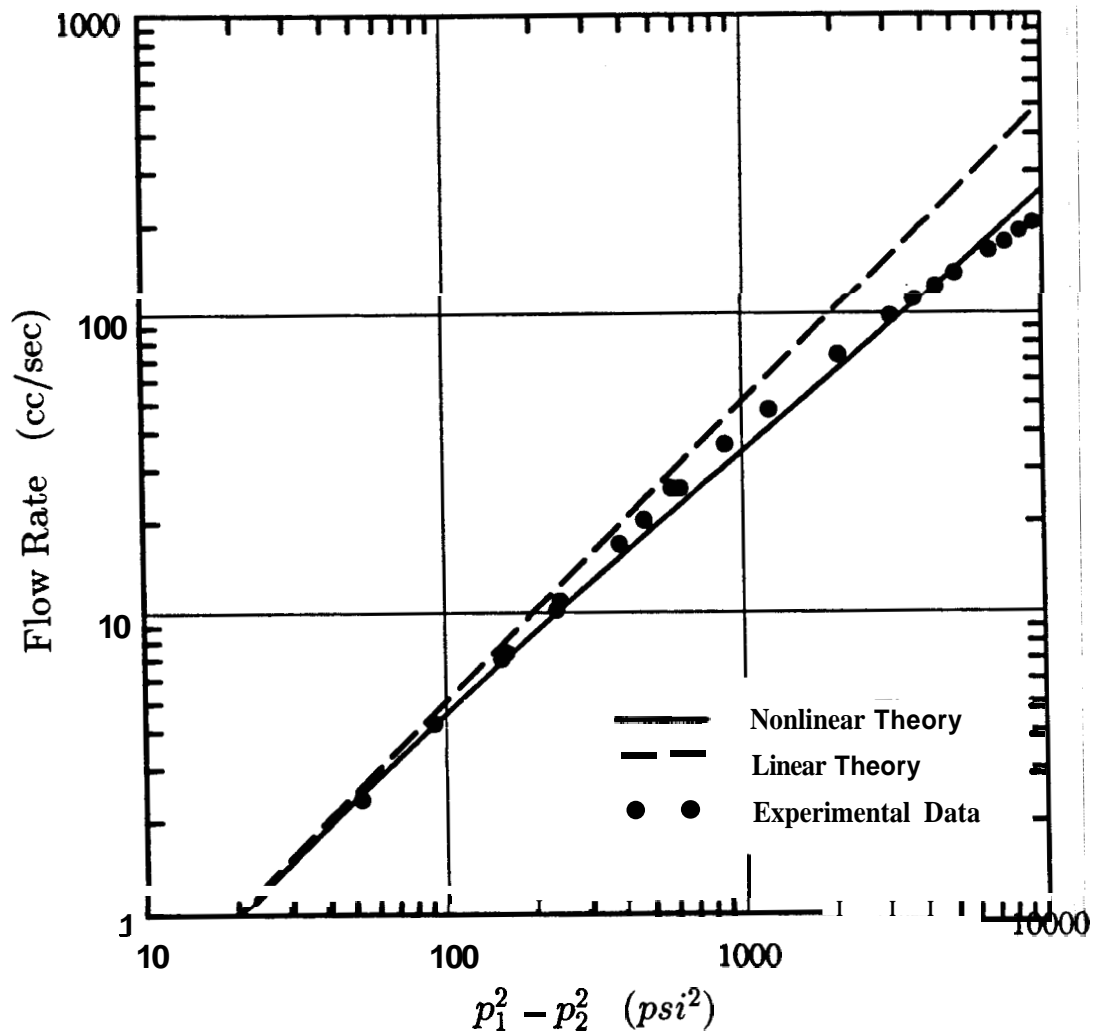


Fig. 3.4 Flow Behavior of Sample 2 of Cornell (1952)

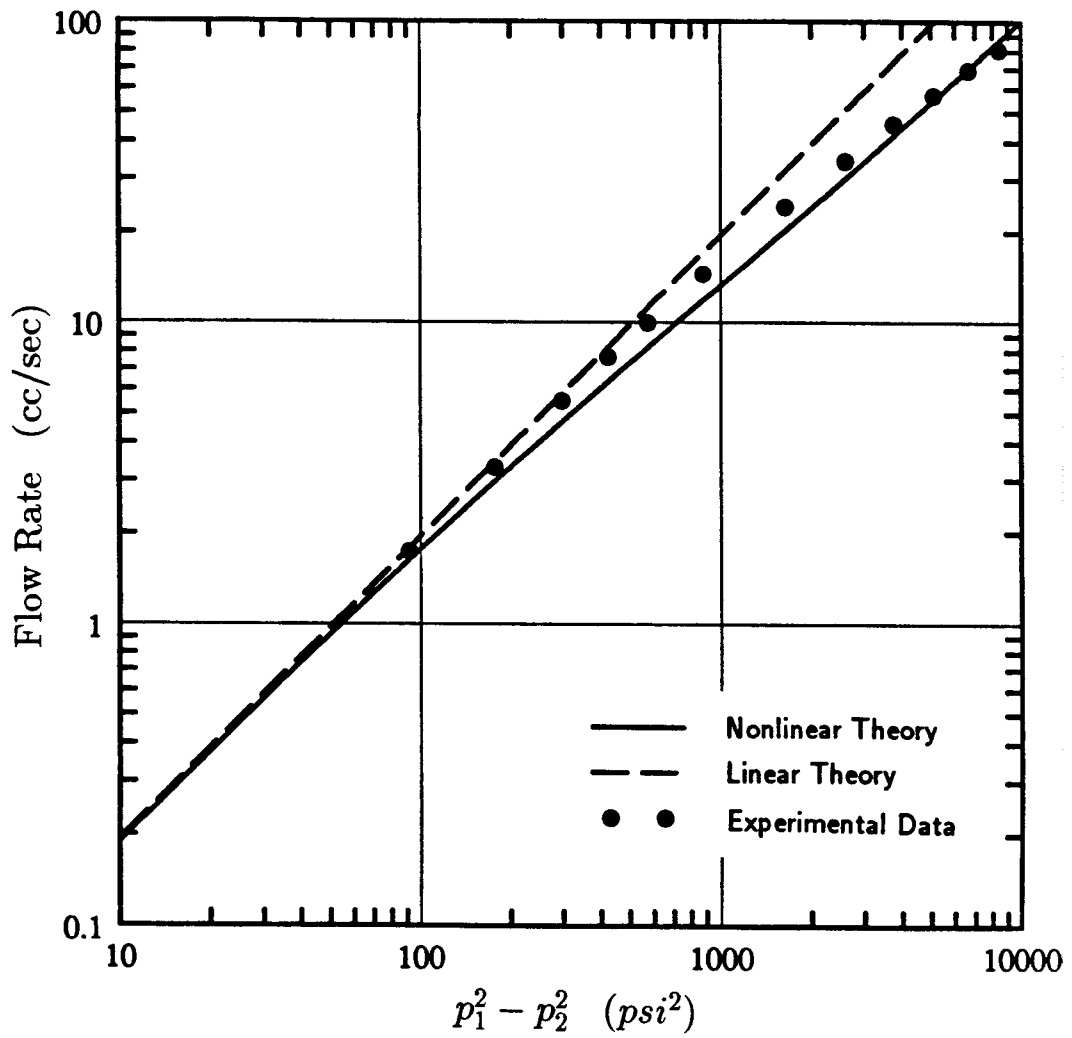


Fig. 3.5 Flow Behavior of Sample 3 of Cornell (1952)

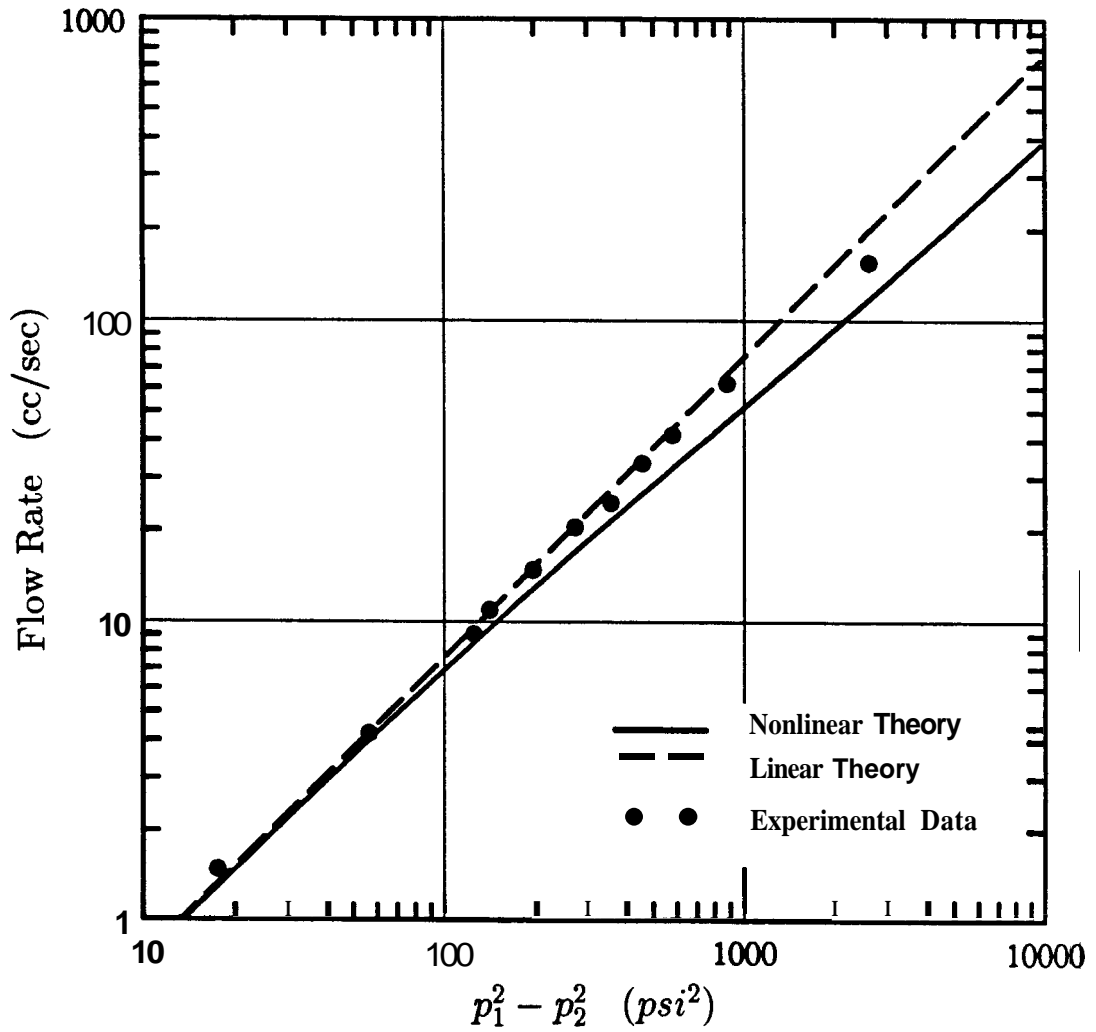


Fig. 3.6 Flow Behavior of Sample 15 of Cornell (1952)

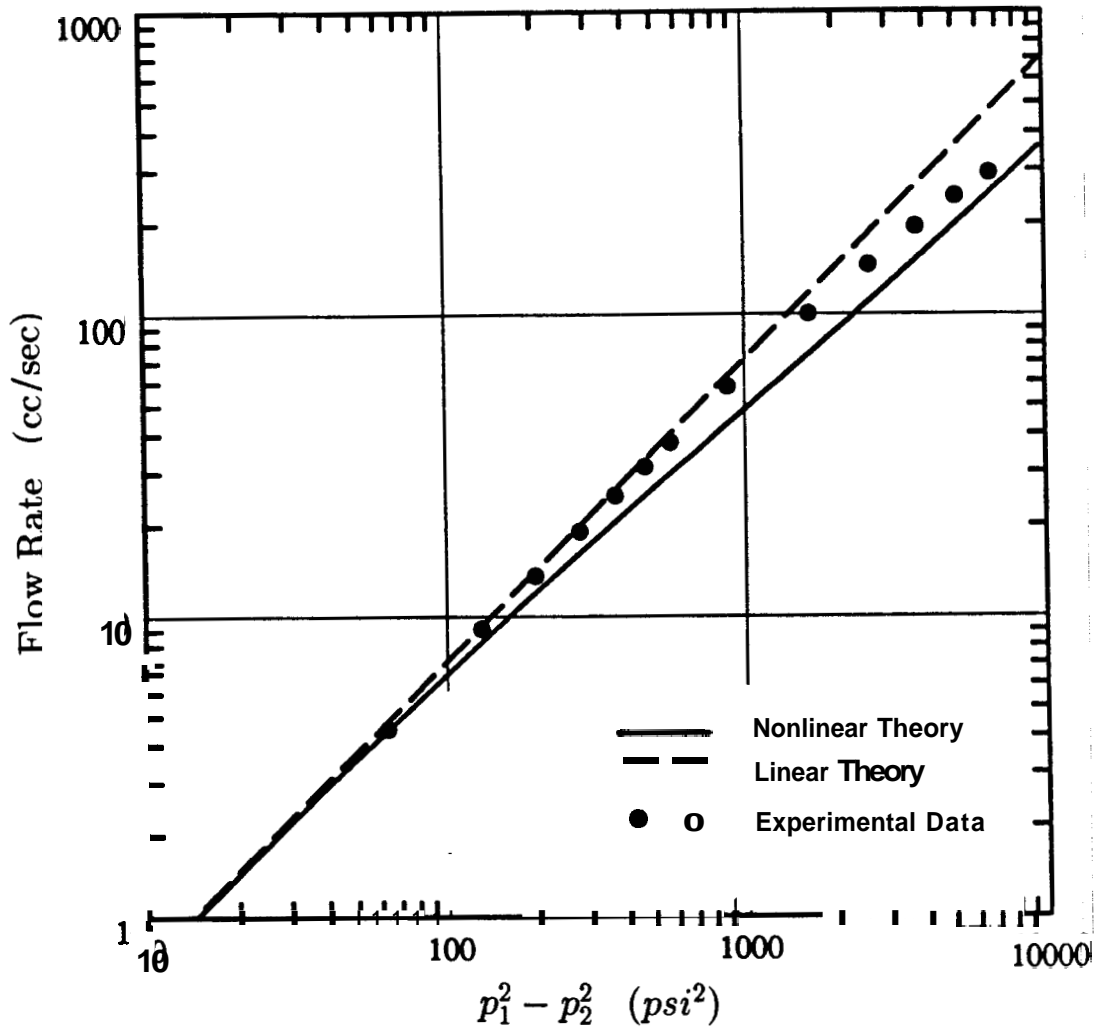


Fig. 3.7 Flow Behavior of Sample 16 of Cornell (1952)

and in the cases of Samples **15** and **16**, the scatter in the plot makes the extrapolation unreliable. The plots used to determine the permeabilities for those two cases are shown in Fig. **3.8**. In both cases, it appears that alternative extrapolations can be performed to arrive at higher permeability values. Figures **3.9** and **3.10** are graphs of flow rate versus squared difference pressure for Samples **15** and **16** respectively, and for permeabilities slightly higher than those reported. The agreement is much better in both the linear and nonlinear regimes, and indicates a high sensitivity of the computed flow rates to permeability.

The analytical model does not match the experimental data exactly within the entire range of pressure drops. This is a result of the fact that an average value is being used to characterize the parameter,  $\bar{c}$ , which is a strong function of pressure. Even with this approximation in the model, the agreement with the experimental data is reasonable.

The good agreement between the analytical model and experimental data confirms the theory that the deviation of flow from linearity is not due to non-Darcy effects but rather to the nonlinearities present in the basic Darcian formulation. This is an important finding. It implies that Darcy's law, in its differential form, is applicable over a wider range of flow rates of than previously thought. While it is possible to have non-Darcy flows at high velocities, the results of this study suggest that the non-Darcy effects cannot be diagnosed on the basis of a simple nonlinear relationship between

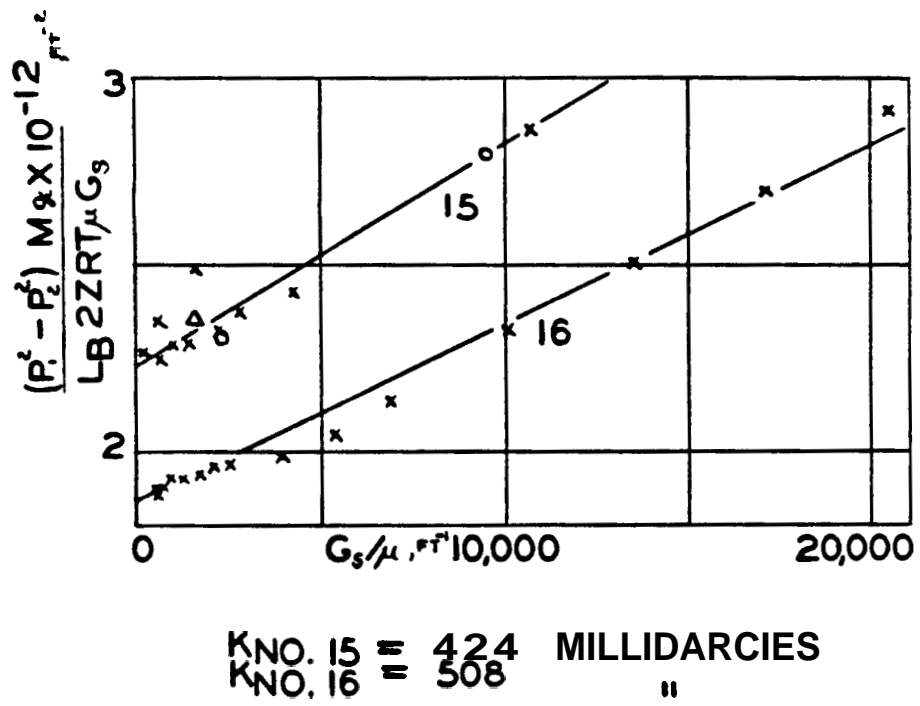


Fig. 3.8 Turbulence Plots for Samples 15 and 16

Cornell (1952)

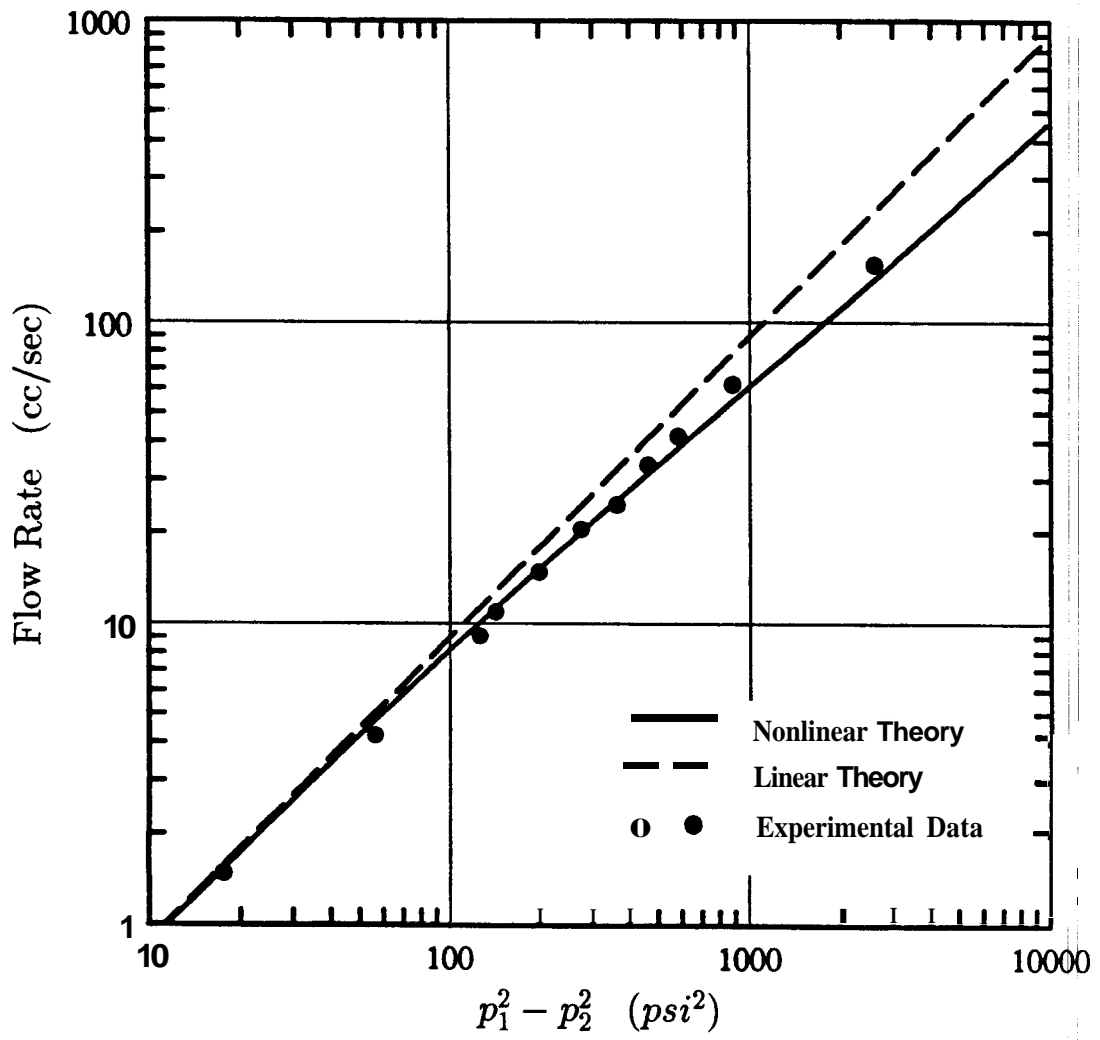


Fig. 3.9 Flow Behavior of Sample 15  
(k=500 md)

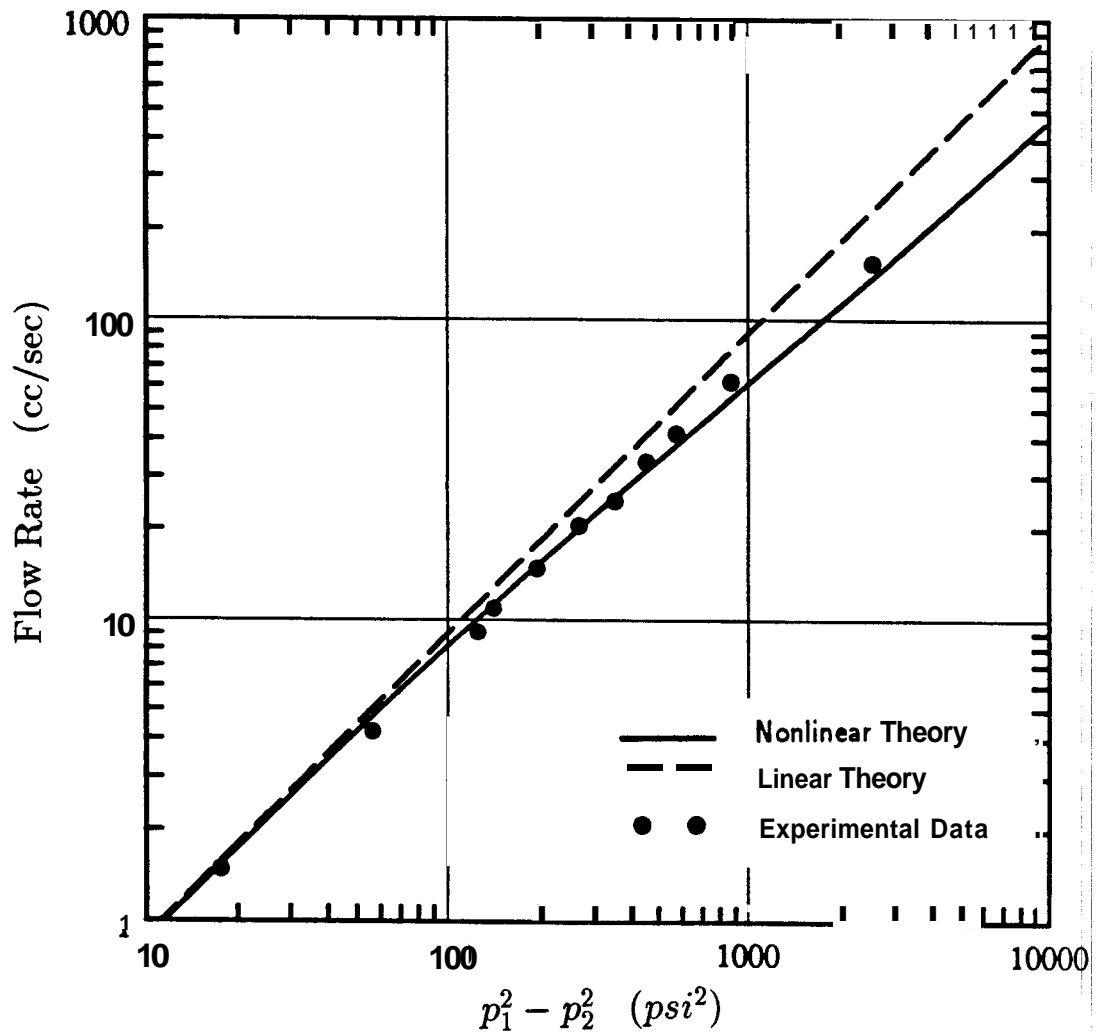


Fig. 3.10 Flow Behavior of Sample 16  
( $k=600$  md)

pressure drop and flow rate.

### 3.2.2 Steady-State Pressure Profile

In this section is derived an equation for determining the steady-state pressure profile in a core. The pressure in this section is nondimensionalized differently from that of the previous section. This is to restrict  $p_D$  to values between 0 and 1, and to allow general inferences to be drawn without having to include the effect of flow rate explicitly. The problem is posed mathematically as follows:

$$\frac{d^2 p_D}{dx_D^2} + \alpha_2 \left( \frac{dp_D}{dx_D} \right)^2 = 0 \quad (3.36)$$

$$p_D = 1 \quad \text{at} \quad x_D = 0 \quad (3.37)$$

$$p_D = 0 \quad \text{at} \quad x_D = 1 \quad (3.38)$$

where:

$$x_D = \frac{x}{L} \quad (3.39)$$

$$p_D = \frac{p(x) - p_2}{p_1 - p_2} \quad (3.40)$$

and

$$\alpha_2 = \bar{c}\Delta p \quad (3.41)$$

The term,  $\alpha_2$ , has a different definition from  $\alpha_1$  of the previous section. While  $\alpha_1$  resulted from a scaling of the problem,  $\alpha_2$  is a consequence of the process of nondimensionalizing, and does not have special physical significance. Thus  $\alpha_2$  can take values much greater than unity depending on the pressure drop and gas compressibility.

The solution for  $\alpha_2 = 0$ , representing the linear problem, is:

$$p_D = 1 - x_D \quad (3.42)$$

The general solution is obtained by making the following substitution:

$$u = \frac{dp_D}{dx_D} \quad (3.43)$$

When Eq. 3.43 is substituted in Eq. 3.36 the differential equation becomes:

$$\frac{du}{dx_D} = -\alpha_2 u^2 \quad (3.44)$$

which has the solution:

$$u = \frac{1}{\alpha_2 x_D + \beta} \quad (3.45)$$

Equation 3.45 may be integrated to yield a solution for  $p_D$  as follows:

$$p_D = \frac{1}{\alpha_2} \ln(\alpha_2 x_D + \beta) + \gamma \quad (3.46)$$

In the preceding equations,  $\beta$  and  $\gamma$  are integration constants which will be determined with the boundary conditions.

When Eqs. 3.37 and 3.38 are applied to Eq. 3.46, the following expressions for  $\beta$  and  $\gamma$  are obtained:

$$\beta = \frac{\alpha_2}{e^{-\alpha_2} - 1} \quad (3.47)$$

$$\gamma = 1 - \frac{1}{\alpha_2} \ln \alpha_2 + \frac{1}{\alpha_2} \ln(e^{-\alpha_2} - 1) \quad (3.48)$$

The equation for  $p_D$  then becomes:

$$p_D = 1 + \frac{1}{\alpha_2} \ln(x_D e^{-\alpha_2} - x_D + 1) \quad (3.49)$$

Equation 3.49 may be written in a compact form by making use of the following identity:

$$1 = \frac{1}{\alpha_2} \ln e^{\alpha_2} \quad (3.50)$$

This results in the following expression for  $p_D$ :

$$p_D = \frac{1}{\alpha_2} \ln(x_D - x_D e^{\alpha_2} + e^{\alpha_2}) \quad (3.51)$$

Figure 3.11 shows a plot of  $p_D$  vs  $x_D$  for various values of  $\alpha_2$ . The plot shows that as expected, the  $\alpha_2 = 0$  line yields a straight line between the end points. The curves for the higher values of  $\alpha_2$  show however, that the profile for a strongly nonlinear system is curved, and the curvature increases with  $\alpha_2$ . The plot shows that for the nonlinear case, most of the pressure drop occurs near the downstream end of the core, and that the average pressure in the system is higher than the arithmetic mean pressure.

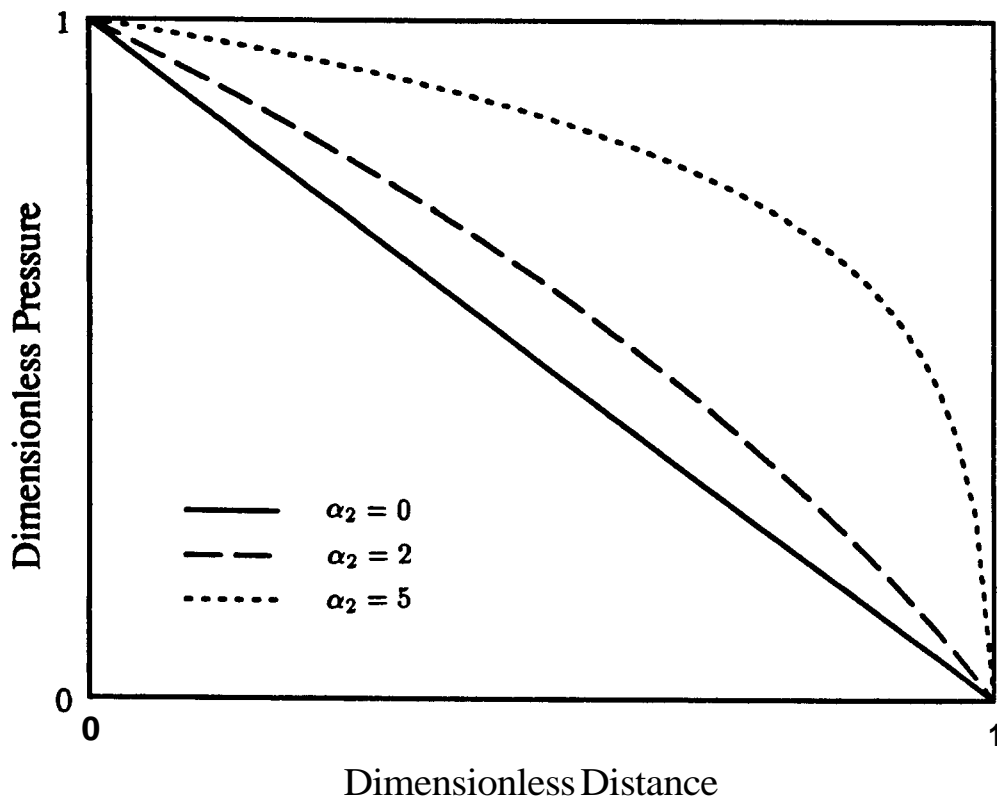


Fig. 3.11 Steady-State Pressure Profiles

### 3.3 Transient Flow

This section deals with the determination of the pressure profiles that are produced during the transient flow of **gas** from one end of a core to the other. Because the interest here is in determining the pressure profiles, the pressure variable is nondimensionalized with respect to the total pressure drop across the core, as in the previous section.

The differential equation representing the transient flow, Eq. 3.1, can be cast in terms of non-dimensional variables as:

$$\frac{\partial^2 p_D}{\partial x_D^2} + \alpha_2 \left( \frac{\partial p_D}{\partial x_D} \right)^2 = \frac{\partial p_D}{\partial t_D} \quad (3.52)$$

where  $p_D$ ,  $x_D$ , and  $\alpha_2$  are defined in Eqs. 3.39, 3.40 and 3.41, and where,

$$t_D = \frac{kt}{\phi \bar{\mu} c_g L^2} \quad (3.53)$$

The compressibility,  $\bar{c}_g$ , and the viscosity,  $\bar{\mu}$ , are evaluated at the mean average pressure of the end faces.

In addition to the boundary conditions specified by Eqs. 3.37 and 3.38, an initial condition is specified as follows:

$$p_D = 0 \quad \text{at} \quad t_D = 0 \quad (3.54)$$

The solution to this problem for the linear case ( $\alpha_2 = 0$ ) is:

$$p_D = (1 - x_D) - \frac{2}{\pi} \sum_{n=1}^{\infty} \frac{1}{n} e^{-n^2 \pi^2 t_D} \sin n\pi x_D \quad (3.55)$$

A solution for the nonlinear case will now be presented.

In order to linearize the equations, the following transformation is effected [Odeh and Babu (1987)]:

$$p_D = \frac{1}{\alpha_2} \ln u \quad (3.56)$$

Substitution of **Eq. 3.56** in **Eq. 3.52** results in the following linear equation:

$$\frac{\partial^2 u}{\partial x^2} - \frac{\partial u}{\partial t_D} \quad (3.57)$$

In terms of the new variable, the initial and boundary conditions become:

$$u = 1 \quad \text{at} \quad t_D = 0 \quad (3.58)$$

$$u = 1 \quad \text{at} \quad x_D = 1 \quad (3.59)$$

$$u = e^{\alpha^2} \quad \text{at} \quad x_D = 0 \quad (3.60)$$

The inhomogeneity present in the boundary conditions is suppressed by expressing the solution,  $u$ , as the sum of a transient part and a steady-state part, viz:

$$u = v(x_D) + w(x_D, t_D) \quad (3.61)$$

Equation 3.57 then becomes:

$$\frac{\partial^2 w}{\partial x_D^2} + \frac{d^2 v}{dx_D^2} - \frac{\partial w}{\partial t} = 0 \quad (3.62)$$

In anticipation of the final result,  $v$  is forced to satisfy the following set of equations:

$$\frac{d^2 v}{dx_D^2} = 0 \quad (3.63)$$

$$v(0) = e^{\alpha^2} \quad (3.64)$$

$$v(1) = 1 \quad (3.65)$$

The solution of Eq. 3.63, subject to Eqs. 3.64 and 3.65 is:

$$v(x) = (1 - e^{\alpha^2})x_D + e^{\alpha^2} \quad (3.66)$$

which is equivalent to the equation for steady flow derived in Section 3.2.

The equations for  $w$  then become:

$$\frac{\partial^2 w}{\partial x_D^2} = \frac{\partial w}{\partial t_D} \quad (3.67)$$

$$w(x_D, 0) = 1 - e^{\alpha^2} + (e^{\alpha^2} - 1)x_D \quad (3.68)$$

$$w(0, t_D) = 0 \quad (3.69)$$

$$w(1, t_D) = 0 \quad (3.70)$$

We assume that  $w$  is separable, i.e. of the **form**:

$$w(x_D, t_D) = X(x_D)T(t_D) \quad (3.71)$$

Upon substitution of Eq. 3.71 in Eq. 3.67, and the separation and solution of the resulting equations, a general equation for  $w$  is obtained as follows:

$$w = e^{-\lambda^2 t_D} (A \cos \lambda x_D + B \sin \lambda x_D) \quad (3.72)$$

The boundary condition of Eq. 3.69 implies that  $A = 0$ . Therefore:

$$w = B e^{-\lambda^2 t_D} \sin \lambda x_D \quad (3.73)$$

From the boundary condition of Eq. 3.70, we have:

$$0 = B e^{-\lambda^2 t_D} \sin \lambda \quad (3.74)$$

This implies that  $\lambda$  takes the following values:

$$\lambda = n\pi, \quad n = 0, 1, 2, \dots \quad (3.75)$$

Since the equations are linear in  $w$ , the general solution for  $w$  is obtained as an infinite sum over  $n$ , as follows:

$$w = \sum_{n=1}^{\infty} B_n e^{-n^2 \pi^2 t_D} \sin n \pi x_D \quad (3.76)$$

Applying the initial condition (Eq. 3.68), an equation for  $B_n$  is obtained. This is:

$$(e^{\alpha^2} - 1)(x_D - 1) = \sum_{n=1}^{\infty} B_n \sin n \pi x_D \quad (3.77)$$

From the theory of Fourier series,  $B_n$  is given by,

$$B_n = 2 \int_0^1 (e^{\alpha^2} - 1)(x_D - 1) \sin n \pi x_D dx_D \quad (3.78)$$

$$= 2 \left( \frac{1 - e^{\alpha^2}}{n \pi} \right) \quad (3.79)$$

Therefore, the complete solution for  $u$  is:

$$u = (1 - e^{\alpha^2})x_D + e^{\alpha^2} + 2(1 - e^{\alpha^2}) \sum_{n=1}^{\infty} \left( \frac{1}{n \pi} \right) e^{-n^2 \pi^2 t_D} \sin n \pi x_D \quad (3.80)$$

This leads to the following expression for  $p_D$ :

$$p_D = \frac{1}{\alpha_2} \ln \left[ (1 - e^{\alpha_2})x_D + e^{\alpha_2} + 2(1 - e^{\alpha_2}) \sum_{n=1}^{\infty} \left( \frac{1}{n\pi} \right) e^{-n^2\pi^2 t_D} \sin n\pi x_D \right] \quad (3.81)$$

Figures 3.12 to 3.17 show a sequence in time of the transient pressure profiles for different values of  $\alpha_2$ . The figures show that increasing values of  $\alpha_2$  result in lower pressure drops at all times. It can also be observed that for all the cases, steady flow conditions are achieved at a dimensionless time of approximately 0.4. Thus, a general equation for predicting the time to steady state is presented as:

$$t_{st} \approx 0.4 \frac{\phi \bar{\mu} c_g L^2}{k} \quad (3.82)$$

Equation 3.82 shows, as expected, that the time to steady-state is high for low permeabilities. It also shows that low pressures, and thus high compressibilities, will result in an increased time to steady state.

The next chapter considers radial flow.

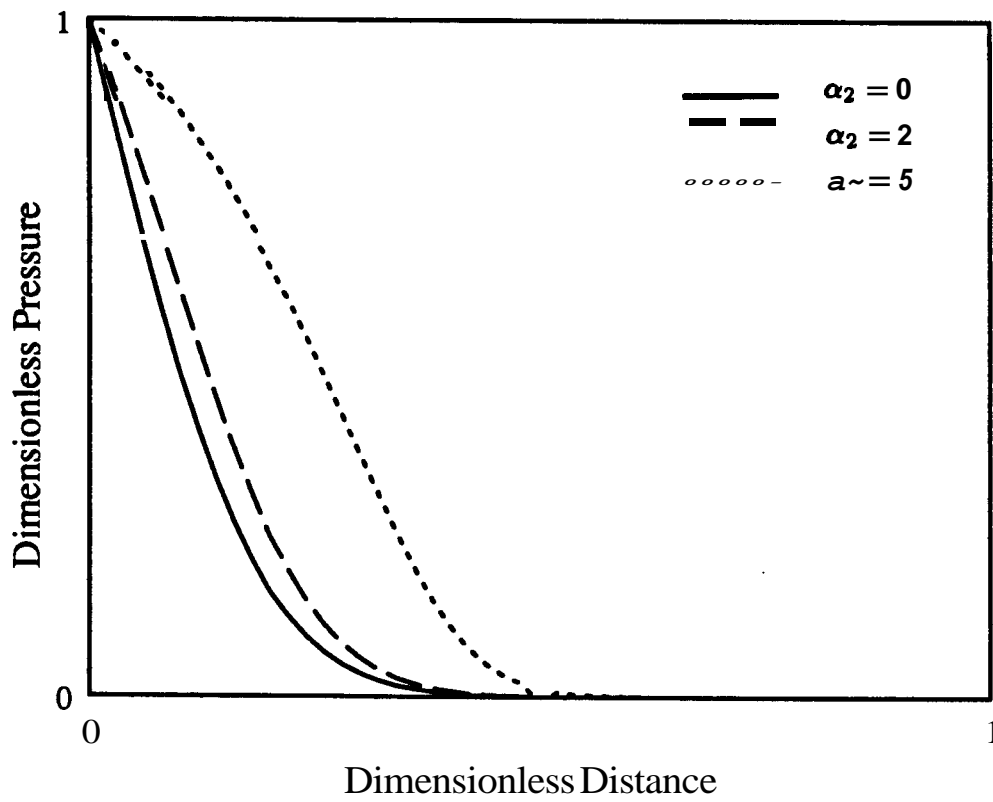


Fig. 3.12 Transient Profiles for  $t_D = 0.01$

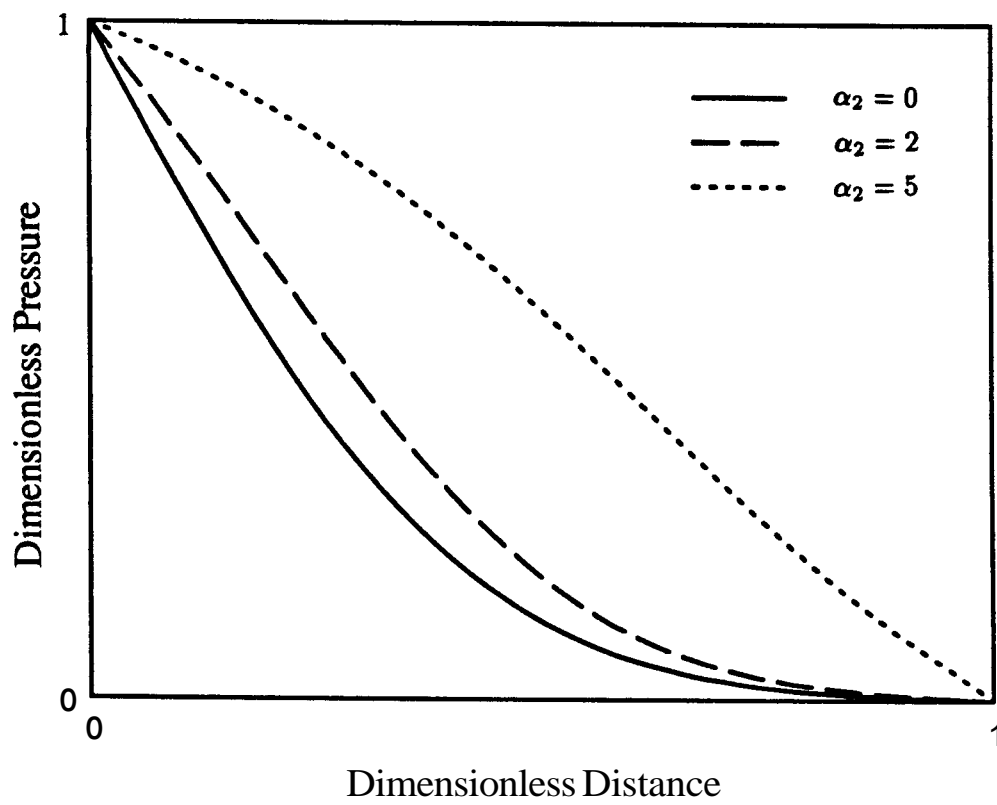


Fig. 3.13 Transient Profiles for  $t_D = 0.05$

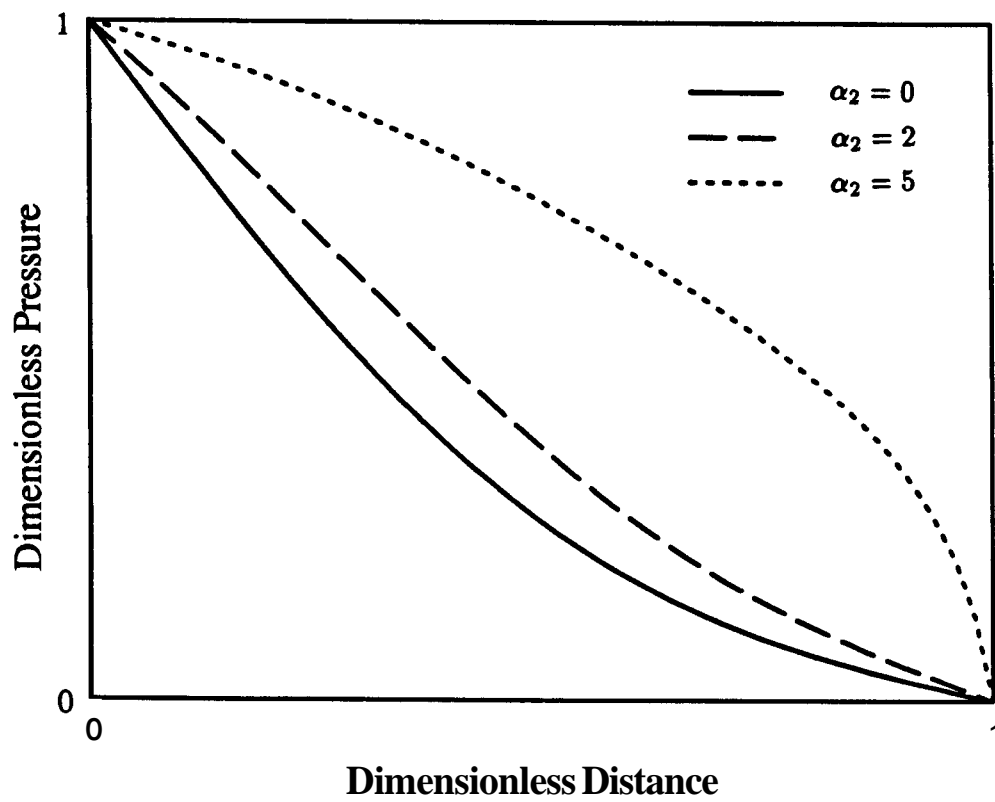


Fig. 3.14 Transient Profiles for  $t_D = 0.1$

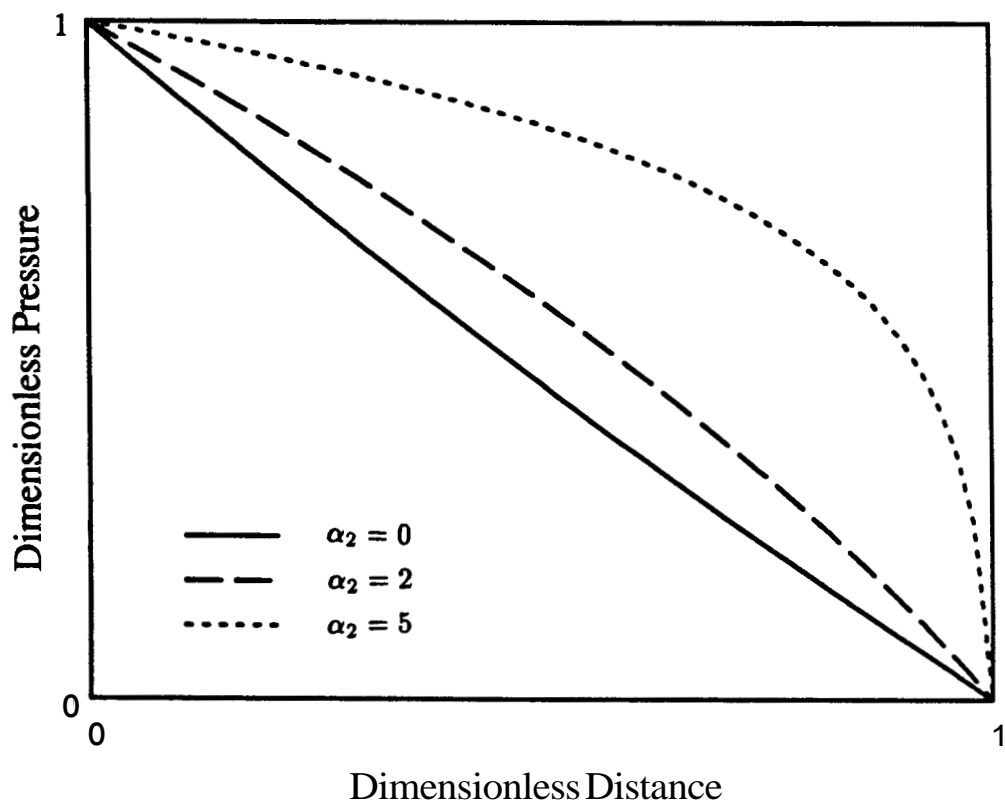


Fig. 3.15 Transient Profiles for  $t_D = 0.3$

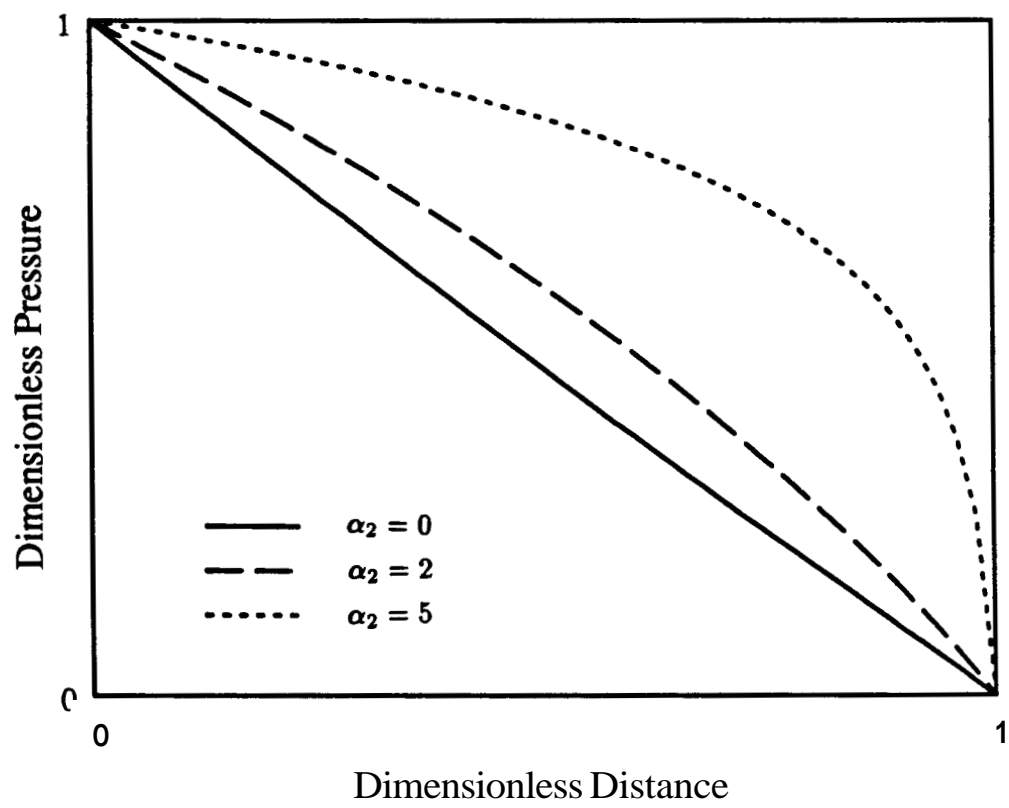
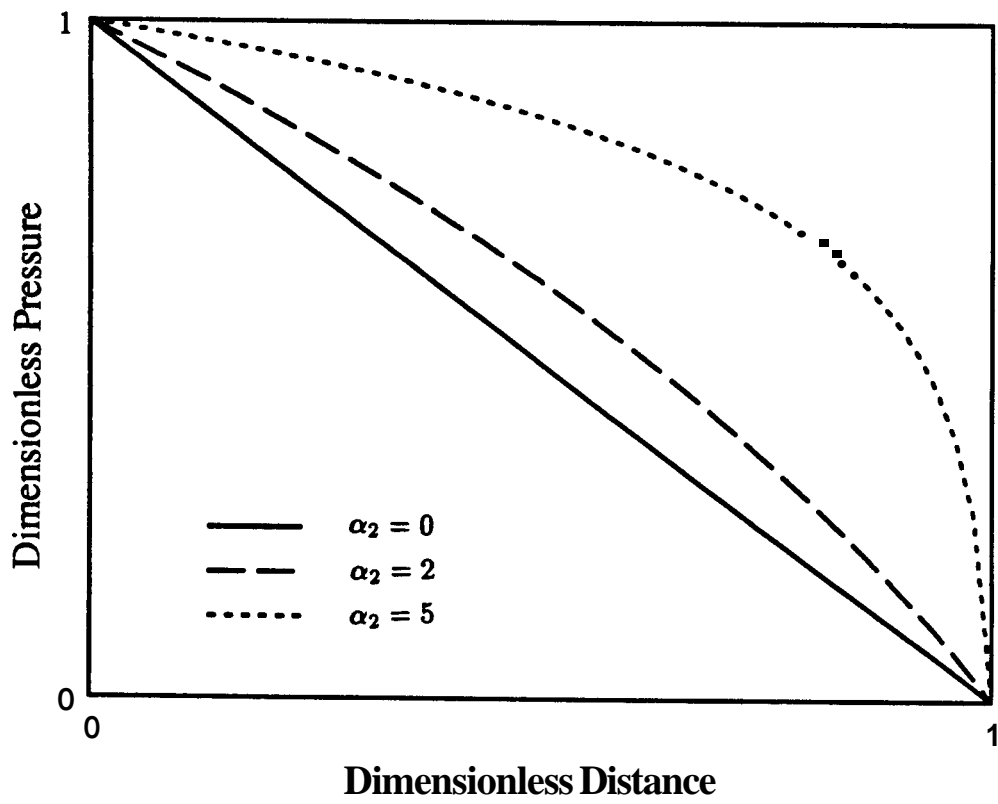


Fig. 3.16 Transient Profiles for  $t_D = 0.4$



**Fig. 3.17** Transient Profiles for  $t_D = 0.5$

# Chapter 4

## Steady Radial Flow

In this chapter, an analysis of the nonlinear, steady, radial flow of gas will be presented. This analysis is of importance because the equation for steady state **flow** is fundamental; all other modes of flow show behavior which can be described in one way or another in forms analogous to the steady flow equation.

In theory, steady flow occurs when there is enough support at the drainage boundary to maintain the pressure at and within the boundary. In practice, a well may 'stabilize' for a period during which it performs in conformity with the steady-state theory. Thus, meaningful predictions and analyses of well performance can, and are made by utilizing the general form of the steady flow equation.

The mathematical problem is formulated in Section 4.1 in terms of squares

of pressure. A solution to the mathematical problem, and discussions of the implications of the results are presented in Section 4.2. Section 4.3 presents analysis and discussion concerning the representation of high rate gas wells in reservoir simulators.

## 4.1 Formulation

The problem was formulated by considering the radial flow of a real gas towards a well producing at a constant surface rate,  $q_{sc}$ . The well was assumed to be completely open to flow in a reservoir of uniform thickness,  $h$ , constant porosity,  $\phi$ , constant permeability,  $k$ , and external radius,  $r_e$ . The effects of skin, wellbore storage, and gravity were ignored.

The partial differential equation describing the flow was derived in Chapter 2, and is presented in terms of squares of pressure as:

$$\frac{\partial^2 p^2}{\partial r^2} + \frac{1}{r} \frac{\partial p^2}{\partial r} - \frac{1}{\mu z} \frac{d(\mu z)}{dp^2} \left( \frac{\partial p^2}{\partial r} \right)^2 = \frac{\phi \mu c}{k} \frac{\partial p^2}{\partial t} \quad (4.1)$$

As was discussed in Chapter 2, the derivation of Eq 4.1 assumes that Darcy's law is valid, and that changes in fluid volumes occur isothermally according to the real gas law.

The boundary condition at the well is merely an application of Darcy's law,

and is given by:

$$r \frac{\partial p^2}{\partial r} = \frac{\mu_w z_w p_{sc} T}{\pi k h T_{sc}} q_{sc} \quad \text{at} \quad r = r_w \quad (4.2)$$

where the subscript,  $w$ , denotes wellbore conditions.

Key to the analysis was the observation that the product  $\mu z$  correlates with pressure according to the relation:

$$\mu z = a + b p^2 \quad (4.3)$$

In Eq. 4.3,  $a$  and  $b$  are constants which are assumed to depend only on temperature and gas composition. This correlation, discussed in Chapter 2, was performed for a range gas gravities and temperatures. Assuming the correlation to be correct, the rate of change of  $\mu z$  with respect to  $p^2$  is:

$$\frac{d(\mu z)}{dp^2} = b \quad (4.4)$$

Figure 4.1 is a graph of the parameter,  $b$ , versus temperature for different gravities of sweet natural gases. The graph shows that  $b$  is large for high gravity gases, and for low temperatures.

When Eq. 4.4 is substituted in Eq. 4.1, the flow equation becomes:

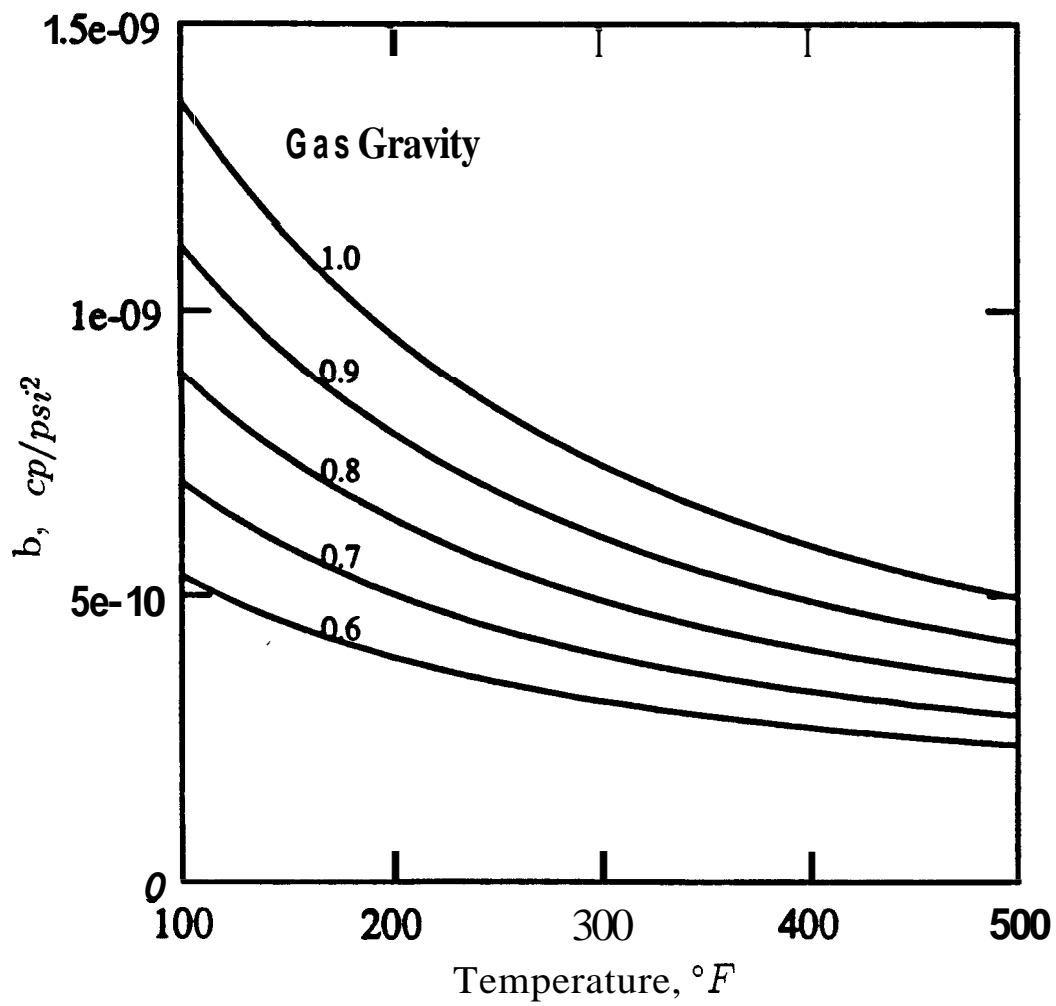


Fig. 4.1 Correlation of 'b' parameter

$$\frac{\partial^2 p^2}{\partial r^2} + \frac{1}{r} \frac{\partial p^2}{\partial r} - \frac{b}{\mu z} \left( \frac{\partial p^2}{\partial r} \right)^2 = \frac{\phi \mu c_t}{k} \frac{\partial p^2}{\partial t} \quad (4.5)$$

We introduce dimensionless variables as follows:

$$p_D = \frac{(p_i^2 - p^2)kh}{1.422(10^6)\mu_i z_i T q_{sc}} \quad (4.6)$$

$$t_D = \frac{0.000264kt}{\phi \mu_i c_{ti} r_w^2} \quad (4.7)$$

$$r_D = \frac{r}{r_w} \quad (4.8)$$

$$r_{eD} = \frac{r_e}{r_w} \quad (4.9)$$

The constants in the dimensionless variables are for English field units. Thus  $q_{sc}$  is in *MMSCFD*,  $t$  is in *hr*,  $k$  is in *md*, and all distances are in feet. The standard pressure and temperature are assumed to have the values **14.7psia** and **520°R** respectively.

When the indicated change in variables is made, **Eq. 4.5** becomes:

$$\frac{\partial^2 p_D}{\partial r_D^2} + \frac{1}{r_D} \frac{\partial p_D}{\partial r_D} + \alpha \left( \frac{\partial p_D}{\partial r_D} \right)^2 = \lambda \frac{\partial p_D}{\partial t_D} \quad (4.10)$$

where:

$$\alpha = \frac{1.422(10^6)Tbq_{sc}}{kh} \left( \frac{\mu_i z_i}{\mu z} \right) \quad (4.11)$$

and:

$$\lambda = \frac{\mu c}{\mu_i c_{ti}} \quad (4.12)$$

The boundary condition at the well is:

$$\frac{\partial p_D}{\partial r_D} = -\sigma \quad \text{at} \quad r_D = 1 \quad (4.13)$$

where:

$$\sigma = \frac{\mu_i z_i}{\mu_w z_w} \quad (4.14)$$

Because  $\mu$ ,  $z$ , and  $c_t$  are functions of pressure, the parameters  $\sigma$ ,  $\lambda$  and  $\alpha$  are in general, pressure-dependent. For true steady flow,  $\sigma$  is constant,

since both  $\mu_i z_i$  and  $\mu_w z_w$  are fixed, and the equations can be solved exactly as posed. In this study it was assumed that both  $\sigma$  and  $\lambda$  are equal to unity, and that the average  $p_a$  is used in place of the initial value. The average values of  $\mu$  and  $z$  are determined at an average pressure defined as,

$$\bar{p} = \sqrt{\frac{p_i^2 + p_w^2}{2}} \quad (4.15)$$

The concern of this work was thus restricted to the nonlinearity due to the squared-gradient term. Since  $\sigma$  is equivalent to a nondimensional well source term, its effect can be accounted for by multiplying all values of  $q_{sc}$  in the resulting equations by  $u$ . The magnitude of  $\sigma$  can be as high as 1.3, and thus ignoring its effect would reduce the effects of flow rate by as much as 30 percent. Kale and Mattar (1980), and Kabir and Hassan (1986) studied the effects of non-unit values of  $\lambda$  on drawdown behavior, and concluded that it results in a small apparent skin factor at the well.

With the foregoing assumptions, the governing equations become:

$$\frac{\partial^2 p_D}{\partial r_D^2} + \frac{1}{r_D} \frac{\partial p_D}{\partial r_D} + \alpha \left( \frac{\partial p_D}{\partial r_D} \right)^2 = \frac{\partial p_D}{\partial t_D} \quad (4.16)$$

$$\frac{\partial p_D}{\partial r_D} = -1 \quad \text{at} \quad r_D = 1 \quad (4.17)$$

where,

$$a = \frac{1.422(10^6)Tbq_{sc}}{kh} \quad (4.18)$$

The significance of the squared-gradient nonlinearity is indicated by the magnitude of  $a$  relative to the other coefficients. Thus deviations from linearity are expected for high flow rates, low values of  $kh$ , high temperatures, and high values of the parameter,  $b$ . A similar parameter dependence was observed in the linear problem described in Chapter 3.

## 4.2 Solution to Steady-State Problem

For true steady flow, the time derivative in **Eq.** 4.16 vanishes, and the equation reduces to:

$$\frac{1}{r_D} \frac{d}{dr_D} \left( r_D \frac{dp_D}{dr_D} \right) + \alpha \left( \frac{dp_D}{dr_D} \right)^2 = 0 \quad (4.19)$$

The inner boundary condition remains unchanged, and an outer boundary condition is introduced to express the fact that the pressure at the boundary is fixed at the initial value. It is:

$$p_D = 0 \quad \text{at} \quad r_D = r_{eD} \quad (4.20)$$

The following variable transformation is effected to make **Eq. 4.19** solvable:

$$u = r_D \frac{dp_D}{dr_D} \quad (4.21)$$

When this substitution is applied, **Eq. 4.19** becomes:

$$\frac{1}{r_D} \frac{du}{dr_D} + \alpha \frac{u^2}{r_D^2} = 0 \quad (4.22)$$

The inner boundary condition also becomes:

$$u = -1 \quad \text{at} \quad r_D = 1 \quad (4.23)$$

The solution to Eqs. **4.22** and **4.23** is:

$$u = \frac{1}{\alpha \ln r_D - 1} = r_D \frac{dp_D}{dr_D} \quad (4.24)$$

Equation **4.24** is integrated with respect to  $r_D$  to give:

$$p_D = \frac{1}{\alpha} \ln [\alpha \ln r_D - 1] + C \quad (4.25)$$

where  $C$  is a constant to be determined from the outer boundary condition, Eq. 4.20. When Eq. 4.20 is applied to Eq. 4.25, we find:

$$C = -\frac{1}{\alpha} \ln [\alpha \ln r_{eD} - 1] \quad (4.26)$$

The complete solution to the problem is then:

$$p_D = \frac{1}{\alpha} \ln \left[ \frac{\alpha \ln r_D - 1}{\alpha \ln r_{eD} - 1} \right] \quad (4.27)$$

By multiplying both the numerator and denominator by  $-1$ , the solution may be expressed in the form:

$$p_D = \frac{1}{\alpha} \ln \left[ \frac{1 - \alpha \ln r_D}{1 - \alpha \ln r_{eD}} \right] \quad (4.28)$$

At the wellbore,  $r_D = 1$ , and Eq. 4.28 reduces to:

$$p_{wD} = -\frac{1}{\alpha} \ln (1 - \alpha \ln r_{eD}) \quad (4.29)$$

In terms of dimensional variables this becomes:

$$p_i^2 - p_w^2 = -\frac{\bar{\mu} \bar{z}}{b} \ln \left( 1 - \frac{1.422(10^6) T b q_{sc}}{k h} \ln(r_e/r_w) \right) \quad (4.30)$$

A deliverability equation was derived by solving for flow rate,  $q_{sc}$  in Eq.

4.30. It is:

$$q_{sc} = \frac{kh}{\ln(r_e/r_w)1.422(10^6)Tb} \left[ 1 - e^{-(p_i^2 - p_w^2) \frac{b}{\mu z}} \right] \quad (4.31)$$

An equation for determining permeability was also derived by a rearrangement of Eq. 4.31:

$$k = \frac{\ln(r_e/r_w)1.422(10^6)Tbq_{sc}}{h \left[ 1 - e^{-(p_i^2 - p_w^2) \frac{b}{\mu z}} \right]} \quad (4.32)$$

To examine the nature of the relationship between flow rate and pressure drop further, Eq. 4.29 was expanded in a Taylor series in  $Q$  as follows:

$$p_{wD} = \ln r_{eD} + \frac{\alpha}{2} \ln^2 r_{eD} + \dots \quad (4.33)$$

The expansion is valid for values of  $\alpha$  and  $r_{eD}$  for which the following relation applies:

$$\alpha \ln r_{eD} < 1 \quad (4.34)$$

A typical value of  $Q$  is of the order of 0.01. Thus the restriction is satisfied

if  $r_{eD}$  is of the order:

$$r_{eD} \sim e^{100} \quad (4.35)$$

For most practical situations this condition is satisfied, and the expansion is valid.

In terms of the original variables, the expansion becomes:

$$p_e^2 - p_w^2 = Aq_{sc} + Bq_{sc}^2 \quad (4.36)$$

where:

$$A = \frac{1.422(10^6)\bar{\mu}zT}{kh} \ln \frac{r_e}{r_w} \quad (4.37)$$

$$B = \frac{2.022(10^{12})\bar{\mu}zT^2}{(kh)^2} \frac{b}{2} \ln^2 \frac{r_e}{r_w} \quad (4.38)$$

$$= A \frac{1.422(10^6)T b}{kh} \frac{1}{2} \ln \frac{r_e}{r_w} \quad (4.39)$$

The 'non-Darcy' coefficient,  $D$ , was artificially introduced by rewriting Eq. 4.36 in the form:

$$p_e^2 - p_w^2 = \frac{1.422(10^6)\bar{\mu}zTq_{sc}}{kh} \left[ \ln \frac{r_e}{r_w} + Dq_{sc} \right] \quad (4.40)$$

By comparing Eq. 4.36 to 4.40, D was determined as follows:

$$D = \frac{1.422(10^6)Tb}{2kh} \ln^2 \frac{r_e}{r_w} \quad (4.41)$$

The preceding developments show that the gradient-squared nonlinearity leads to a pressure drop and flow relationship which is nonlinear, and is of a form which is usually attributed to deviations from Darcy's law. This suggests the likelihood, as in the linear flow case, that these deviations are not due to non-Darcy flow, but result from neglecting gradient squared terms. The equations derived here thus make it possible to compute high rate well performance without resorting to empirically-derived coefficients.

As expected, the additional pressure drop is large for low permeability formations, and for high flow rates or pressure gradients. It is also a function of the drainage radius, although weakly so, a fact which is not usually considered in the analysis of high rate flow. This dependence on drainage area suggests that in the transient problem, the quadratic and higher order terms will be a function of time, since drainage radius increases with time. Presently, it is theorized [Lee(1982)] that the effect of time on the pressure drop is manifested only in the linear term. This issue is addressed in greater

detail in Chapter 6.

An example problem is discussed in Chapter 5 to examine the magnitude of the nonlinear quadratic term compared to the linear term.

### 4.3 Simulation of High Rate Gas Wells

The results obtained in the previous section have implications for the simulation of high rate gas wells. The designation ‘high rate wells’ is used here to refer to those wells and rates for which pressure drop and flow relate in a significantly non-linear fashion.

One of the problems in the treatment of wells in reservoir simulators is how to relate the wellbore pressure to the computed pressure of the gridblock containing the well. The well flow rate of a phase is usually determined as the product of the pressure drop between the well and the gridblock, the phase mobility at the wellbore, and a geometric factor. Thus, for single phase, horizontal flow:

$$q_j = \lambda_j G_j (p_j - p_w) \quad (4.42)$$

where:

$$\lambda_j = \frac{k}{\mu_w B_w} \quad (4.43)$$

$G_j$  is a geometric factor for the gridblock, and is related to the block shape and size, and the location of the well in the block. The geometric factor is the term through which the wellbore and gridblock pressures are related.

Usually single well radial models are constructed with closely-spaced grids near the well. The goal is to account for the rapid changes that occur near the well correctly, and to reduce computation cost farther from the well, where pressure gradients are small. For such a method, the geometric factor follows directly from the radial differencing procedure. Assuming steady-state flow between the block and the well, the geometric factor is:

$$G_j = \frac{C \Delta z_j}{\frac{r_2^2}{r_2^2 - r_1^2} \ln \frac{r_2}{r_1} - \frac{1}{2} + s} \quad (4.44)$$

where  $r_1$  is the well radius,  $r_2$  the radius of the gridblock, and  $\Delta z_j$  is the vertical section open to flow. The constant,  $C$ , depends of the units employed, and the term,  $s$ , is a skin factor to model damage or other restrictions to flow near the wellbore.

To account for high rate, nonlinear flow of free gas, a flow-dependent skin factor is usually added to the damage skin factor,  $s$ . This rate-dependent skin factor is defined as:

$$s_1 = Dq_j \quad (4.45)$$

where the  $D$  is specified by the user of the simulator, and is determined from either correlations or well tests. An alternative way to account for nonlinear gas flow has been to use the backpressure equation.

This study has concluded, however, that for the radial flow situation described, it may be unnecessary and incorrect to include terms to account for 'turbulence'. This is because the grids near the well are usually fine enough to account for the changes in fluid properties correctly which may cause the nonlinear behavior. If on the other hand, there is a strong evidence of actual non-Darcy effects, then they must be included in the model. But as we have demonstrated, that evidence cannot be based merely on an observed nonlinearity between pressure drop and flow rate.

The representation of wells in rectangular grids presents a different problem. In this situation, the well behavior is predicted on the basis of the pressure of a grid block whose dimensions are large compared to those of the well. The problem in this case is to account for the radial flow near a well within a rectangular grid system.

Peaceman [1978, 1983] and Abou-Kassem and Aziz (1985) have studied the problem of modelling oil wells in rectangular grids. Peaceman's results were extended in this study to suggest procedures for modeling gas wells,

particularity those flowing at high rates.

Peaceman (1978) defined an equivalent radius,  $r_e$ , at which the steady-state well flowing pressure is equal to the well block pressure computed by the simulator. For liquid flow, the equation, in Darcy units, is:

$$p_o - p_w = \frac{\mu q}{2\pi k h} \ln(r_o/r_w) \quad (4.46)$$

where  $p_o$  is the simulator computed grid block pressure, and  $r_e$  is the associated equivalent radius.

For square grids, Peaceman [1978] showed that  $r_e$  is related to  $\Delta x$ , the grid linear dimension, by the simple equation:

$$r_e = 0.2\Delta x \quad (4.47)$$

For non-square, isotropic grids, Peaceman [1983] showed that

$$r_e = 0.14\sqrt{\Delta x^2 + \Delta y^2} \quad (4.48)$$

For modeling gas wells, Peaceman suggested the use of the gas pseudo-pressure,  $m(p)$ , in place of pressure in his equations. This approach is the recommended method because for steady-state flow, the gas flow equation

in terms of  $m(p)$  is identical in form to the pressure equation for incompressible liquid flow, which formed the basis of Peaceman's derivations. The geometric factor for a rectangular grid can be defined as:

$$G_j = \frac{\Delta z_j}{\ln \frac{r_e}{r_w} + s} \quad (4.49)$$

where again the factor,  $s$ , accounts for physical restrictions to flow. As in the radial case, the modeling of nonlinear gas flow has been accomplished by either the inclusion of a rate-dependent skin factor, or the application of the backpressure equation.

If one chooses to perform the analysis in terms of squares of pressure then the results of this study can be combined with Peaceman's work as follows. Peaceman's derivation assumed that the Laplace equation describes the flow between the grid block containing the well and the four adjacent blocks. For steady gas flow analysis based the squared-pressure formulation, the Laplace equation is not strictly applicable because of the presence of the gradient-squared term. However, as has been shown in this work, the effect of the nonlinearity of the flow equation is localized in the vicinity of the well. Thus for interblock flow, the Laplace equation (in terms of squares of pressure) is a good approximation. Even with that approximation, direct application of Peaceman's procedure to the results of this study would lead to an equivalent radius,  $r_o$ , that is a function of gas flow rate.

An alternative, approximate approach is as follows. For a rate specified well, Eq 4.30 is used to compute well pressure in the simulator by replacing  $r_e$  by  $r_o$ , and  $p_e$  by  $p_j$ , where  $p_j$  is the simulator block pressure, and  $r_o$  is the equivalent radius defined by Peaceman. Thus, in English field units:

$$p_w^s \equiv p_j^s + \mu_j z_j \ln \left( 1 - \frac{1.422(10^6) T b q_{sc}}{k h} \ln(r_o/r_w) \right) \quad (4.50)$$

For bottomhole pressure specification, Eq. 4.31 can be used to derive an equation for computing flow rate. This is:

$$q_{sc} = \frac{k h}{\ln(r_o/r_w) 1.422(10^6) T b} \left[ 1 - e^{(r_j - p_w^2) \frac{b}{\mu_j z_j}} \right] \quad (4.51)$$

These nonlinear terms are necessary not because Darcy's law is invalid, but because the choice has been made to model wells in finite grids in terms of pressures rather than the  $m(p)$  function.

A better method for simulating gas wells in rectangular grids is to use a hybrid grid system. This method is described by Pedrosa and Aziz [1987], and involves the imposition of a radial grid within the rectangular grid block containing the well. As in the purely radial grid case, there would be no need to include nonlinear terms to account for 'turbulence' if the radial grids are fine enough.

---

We consider stabilized radial flow in the following. The term “stabilized” is used to describe flow similar to pseudosteady state for a constant rate liquid flow from a closed outer boundary system.

# Chapter 5

## Stabilized Flow

The analysis of nonlinear radial flow is continued in this chapter with the consideration of stabilized flow. Stabilized flow is a condition similar to pseudo-steady liquid flow, and is attained after the well has produced long enough, at a constant surface rate, to produce from the entire drainage radius. Theoretically, pseudo-steady flow is possible only under conditions of constant and small compressibilities. Thus, strictly speaking, pseudo-steady flow is not possible in gas reservoirs where the compressibilities are strong functions of pressure. Nevertheless, the concept is still widely applied to gas reservoirs, and many deliverability analyses are based on equations similar to those for pseudo-steady liquid equations, [ERCB (1975)].

In the following sections, the nonlinear stabilized flow problem will be formulated, and the solution derived. A perturbation series method will be

used to solve the problem. The series method is used since the exact solution is difficult to obtain, and because the series solution exhibits features that are of interest in this study. A numerical example will also be presented to demonstrate the applicability of the results obtained.

## 5.1 Formulation

The general dimensionless equation for the radial flow of gas was presented in Chapter 4. It is:

$$\frac{\partial^2 p_D}{\partial r_D^2} + \frac{1}{r_D} \frac{\partial p_D}{\partial r_D} + \alpha \left( \frac{\partial p_D}{\partial r_D} \right)^2 = \frac{\partial p_D}{\partial t_D} \quad (5.1)$$

If stabilized flow conditions are assumed, then by analogy with pseudosteady liquid flow, the pressure is expected to behave according to the following equation:

$$p_D = \frac{2t_D}{r_e^2} + f(r_D) \quad (5.2)$$

The first term in Equation 5.2 represents the voidage of the reservoir with time, and the second term describes the variation of pressure with location within the reservoir. As shown by Ramey and Cobb [1971],  $f(r_D)$  is equivalent to a dimensionless pressure based on average pressure, instead of the

initial pressure. That is:

$$f(r_D) = \frac{(\bar{p}^2 - p^2)}{1.422(10^6)\mu z T q_{sc}} \quad (5.3)$$

Al-Hussainy (1967) discussed the meaning of the average pressure during stabilized gas flow, and stated that the average pressure is not a volumetric average, but rather the static pressure following a complete pressure build-up. The difference between the two average pressures is small, however, and the average pressure can be described mathematically as an average over the reservoir volume with small error.

Upon substitution of Eq. 5.2 in Eq. 5.1, an equation in terms of  $f(r_D)$  results as follows:

$$\frac{d^2 f}{dr_D^2} + \frac{1}{r_D} \frac{df}{dr_D} + \alpha \left( \frac{df}{dr_D} \right)^2 = \frac{2}{r_{eD}^2} \quad (5.4)$$

The boundary condition at the well is:

$$\frac{df}{dr_D} = -1 \quad \text{at} \quad r_D = 1 \quad (5.5)$$

The outer boundary condition is an expression of the fact that the volumetric average pressure as used as a reference. This is:

$$\int_1^{r_{eD}} r_D f dr_D = 0 \quad (5.6)$$

Equation 5.6 is derived from the definition:

$$\bar{p} = \frac{\int_{V_w}^{V_e} p dV}{\int_{V_w}^{V_e} dV} \quad (5.7)$$

Or:

$$\bar{p} = \frac{\int_{r_w}^{r_e} r p dr}{\int_{r_w}^{r_e} r dr} \quad (5.8)$$

and therefore:

$$\frac{\int_{V_w}^{V_e} (\bar{p} - p) dV}{\int_{V_w}^{V_e} dV} = 0 \quad (5.9)$$

or:

$$\frac{\int_{r_w}^{r_e} (\bar{p} - p) r dr}{\int_{r_w}^{r_e} r dr} = 0 \quad (5.10)$$

## 5.2 Solution of Stabilized Flow Problem

A two-term series expansion solution of the nonlinear stabilized flow problem is presented in this section. The method used to determine the terms in the series is that of ‘parametric differentiation’ [Lin and Segel (1974)]. The underlying basis of the method is that  $f(r_D)$  can be expressed in a Taylor series in  $a$ . The coefficients of the terms in the series are then given by the successively higher order differentials of  $f(r_D)$  with respect to  $\alpha$ , as  $a$  tends to zero in the limit.

It is assumed that  $f$  has derivatives with respect to  $\alpha$ , and that both  $f$  and  $\partial f/\partial \alpha$  have limits  $f_0$  and  $f_1$  respectively as  $a$  tends to zero.

To obtain the first term in the expansion, we let  $\alpha = 0$  in the limit. Equations 5.4, 5.5 and 5.6 then become:

$$\frac{d^2 f_0}{dr_D^2} + \frac{1}{r_D} \frac{df_0}{dr_D} = \frac{2}{r_{eD}^2} \quad (5.11)$$

$$\frac{df_0}{dr_D} = -1 \quad \text{at} \quad r_D = 1 \quad (5.12)$$

$$\int_1^{r_{eD}} r_D f_0 dr_D = 0 \quad (5.13)$$

This is the classical linear problem, and has the solution:

$$f_0 = \frac{1}{2} \frac{r_D^2}{r_{eD}^2} + \ln \frac{r_{eD}}{r_D} - \frac{3}{4} \quad (5.14)$$

The second term may be obtained by differentiating Eqs. 5.4, 5.5 and 5.6 with respect to  $\alpha$  to obtain:

$$\frac{1}{r_D} \frac{\partial}{\partial \alpha} \left[ \frac{d}{dr_D} \left( r_D \frac{df}{dr_D} \right) \right] + \left( \frac{df}{dr_D} \right)^2 + 2\alpha \left( \frac{df}{dr_D} \right) \left( \frac{\partial f}{\partial \alpha} \right) = 0 \quad (5.15)$$

$$\frac{\partial}{\partial \alpha} \left( \frac{df}{dr_D} \right) = 0 \quad \text{at} \quad r_D = 1 \quad (5.16)$$

$$\frac{\partial}{\partial \alpha} \int_1^{r_{eD}} r_D f dr_D = 0 \quad (5.17)$$

When  $\alpha$  is made to approach zero in the limit, the equations for  $f_1$  may be obtained as follows:

$$\frac{1}{r_D} \frac{d}{dr_D} \left( r_D \frac{df_1}{dr_D} \right) + \left( \frac{df_0}{dr_D} \right)^2 = 0 \quad (5.18)$$

$$\frac{df_1}{dr_D} = 0 \quad \text{at} \quad r_D = 1 \quad (5.19)$$

$$\int_1^{r_{eD}} r_D f_1 dr_D = 0 \quad (5.20)$$

When  $f_0$ , given by Eq. 5.14, is substituted in Eq. 5.18, the differential equation for  $f_1$  becomes:

$$\frac{1}{r_D} \frac{d}{dr_D} \left( r_D \frac{df_1}{dr_D} \right) = \frac{2}{r_{eD}^2} - \frac{1}{r_D} - \frac{r_D^2}{r_{eD}^2} \quad (5.21)$$

Equation 5.21 may be solved by successive integration as follows:

When both sides of Eq. 5.21 are multiplied by  $r_D$ , the equation becomes:

$$\frac{d}{dr_D} \left( r_D \frac{df_1}{dr_D} \right) = \frac{2r_D}{r_{eD}^2} - \frac{1}{r_D} - \frac{r_D^3}{r_{eD}^2} \quad (5.22)$$

Equation 5.22 is integrated with respect to  $r_D$  to yield:

$$r_D \frac{df_1}{dr_D} = \frac{r_D^2}{r_{eD}^2} - \ln r_D - \frac{1}{4} \frac{r_D^4}{r_{eD}^2} + c_1 \quad (5.23)$$

where  $c_1$  is an integration constant, and may be determined by applying Eq. 5.19, the well boundary condition. When Eq. 5.19 is applied to Eq. 5.23, we find:

$$c_1 = 0 \quad (5.24)$$

Equation 5.23 may be integrated to obtain  $f_1$  as follows:

$$f_1 = \frac{1}{2} \frac{r_D^2}{r_{eD}^2} - \frac{1}{2} \ln^2 r_D - \frac{1}{16} \frac{r_D^4}{r_{eD}^2} + c_2 \quad (5.25)$$

The integration indicated by Eq. 5.17 may be performed on **Eq. 5.25** to determine  $c_2$ , the integration constant, as:

$$c_2 = \frac{13}{48} + \ln^2 r_{eD} - \ln r_{eD} \quad (5.26)$$

The complete solution for  $f_1$  is:

$$f_1 = \frac{1}{2} \frac{r_D^2}{r_{eD}^2} - \frac{1}{2} \ln^2 r_D - \frac{1}{16} \frac{r_D^4}{r_{eD}^2} + \frac{13}{48} + \ln r_{eD} - \ln r_{eD} \quad (5.27)$$

In deriving Eq. 5.27, all terms of the order  $1/r_{eD}^2$  and lower were neglected. This assumption is reasonable since  $r_{eD}$  is of the order of 5000 for a typical gas well.

If the constant  $13/48$  is further approximated by  $1/4$ , **Eq. 5.27** becomes:

$$f_1 = \frac{1}{8} \frac{r_D^2}{r_{eD}^2} - \frac{1}{2} \ln r_D - \frac{1}{16} \frac{r_D^4}{r_{eD}^2} + \left( \ln r_{eD} - \frac{1}{2} \right)^2 \quad (5.28)$$

The finite Taylor series expansion of  $f_D$  in  $a$  is then,

$$f(r_D; \alpha) = f_0(r_D) + \alpha f_1(r_D) \quad (5.29)$$

where  $f_0$  and  $f_1$  are given by Eqs. 5.19 and 5.28 respectively.

At the wellbore, where  $r_D = 1$ , the pressure drop is:

$$f_w = \left( \ln r_{eD} - \frac{3}{4} \right) + \alpha \left( \ln r_{eD} - \frac{1}{2} \right)^2 \quad (5.30)$$

Equation 5.30 may be expressed in terms of dimensional variables by recalling the definitions of  $a$  and  $f$  from Eqs. 4.17 and 5.3 respectively:

$$\bar{p}^2 - p_w^2 = A_1 q_{sc} + B_1 q_{sc}^2 \quad (5.31)$$

where:

$$A_1 = \frac{1.422(10^6) \bar{\mu} z T}{kh} \left[ \ln \frac{r_e}{r_w} - \frac{3}{4} \right] \quad (5.32)$$

and:

$$B_1 = \frac{2.022(10^{12})\overline{\mu z}T^2b}{(kh)^2} \left[ \ln \frac{r_e}{r_w} - \frac{1}{2} \right]^2 \quad (5.33)$$

This can be expressed in the alternative form, involving the D coefficient:

$$\overline{p}^2 - p_w^2 = \frac{1.422(10^6)\overline{\mu z}T}{kh} \left[ \ln \frac{r_e}{r_w} - \frac{3}{4} + Dq_{sc} \right] \quad (5.34)$$

with the coefficient,  $D$ , defined as:

$$D = \frac{1.422(10^6)Tb}{kh} \left[ \ln \frac{r_e}{r_w} - \frac{1}{2} \right]^2 \quad (5.35)$$

This result shows again that an effect of the nonlinearity in the differential equation is a nonlinear relationship between pressure drop and flow rate. This relationship, of the Forchheimer type, is usually interpreted as an indication of deviation from Darcy flow. Clearly, since a basis of our analysis is Darcy's law, the deviation from linearity is due to the effects of the gradient-squared term, and is not a 'non-Darcy' effect.

As in the steady flow case, the coefficient of the nonlinear term is a function of reservoir size, in contradiction of current theory. The effect of reservoir size is tempered however, by the logarithm, and thus does not affect the coefficient as much as do other parameters (for example,  $kh$ ). Thus a deviation from linearity between flow rate and pressure drop cannot be

used as conclusive evidence of non-Darcy flow, as has been the practice.

A gas deliverability problem will be presented here to illustrate the use of the equations, to obtain an indication of the magnitude of the terms, and to compare with results computed by another method. The example is taken from pp. 7-19 of ERCB [1975]. In this example it is assumed that the well has a zero skin factor, instead of that of  $-2$  used in the original problem.

Given the following gas and reservoir properties, we wish to establish the stabilized deliverability potential of the well.

- $\bar{\mu} = 0.02cp$
- $\bar{z} = 0.81$
- $\gamma_g = 0.78$
- $T = 630^\circ R$
- $k = 14md$
- $h = 45ft$
- $r_w = 0.3ft$
- $r_e = 2600ft$
- $S=0$

Equation 5.31 may be used to compute the stabilized deliverability of the well. To use Eq. 5.31 an estimate of the parameter,  $b$ , is required. Figure 5.1 is a graph of  $b$  versus temperature for different values of gas gravity. Using the given reservoir temperature and gas gravity, a value of  $b$  may be read directly from the figure:

$$b = 6.8(10^{-10})cp/psia^2$$

$A_1$  and  $B_1$  are then calculated from Eqs. 5.32 and 5.33 respectively to give:

$$A_1 = 191,600$$

$$B_1 = 1,635$$

The stabilized deliverability equation is then:

$$\bar{p}^2 - p_w^2 = 191,600q_{sc} + 1,635q_{sc}^2$$

The value of  $B_1$  is of the same order of magnitude as that calculated in the book [ERCB (1975)], which was 2,510. Their value was calculated from Swift and Kiel's [1962] equation, which involves the non-Darcy parameter,  $\rho$ , obtained from correlations of experimental results. If the well

were to produce at  $100\text{MMSCFD}$ , the linear component of the pressure drop would be  $1.1916(10^7)\text{ psi}^2$ , and the nonlinear contribution would be  $1.635(10^6)\text{ psi}^2$ . The two components would both be significant.

This example shows that the extra pressure drop resulting from the nonlinear squared-gradient term can be large, and compares with that computed by other methods based on the assumption of non-Darcy flow. The observed deviations that have been attributed to non-Darcy flow may be a result of the gradient-squared nonlinearity of the governing differential equation.

The next chapter considers transient flow in an infinitely large reservoir.

## Chapter 6

# Transient Radial Flow

This chapter is concerned with the analysis of the unsteady nonlinear flow towards a well in an infinite-acting system. The infinite-acting model represents the period before the effects of external boundaries are felt.

The results to be presented here relate to the pressure responses during drawdown and injection. The analysis of the steady radial problem in Chapter 3 revealed that the coefficients of the nonlinear rate terms in the pressure solution are functions of drainage radius. Since in unsteady flow, the drainage radius increases with time, it is expected that the coefficients of all the rate terms in the transient problem will be time-dependent. This would seem to contradict prevailing theories, which suppose that the time-dependency is confined only to the linear term (Lee, 1982).

## 6.1 Drawdown

The following is a derivation of the equation for the pressure response due to a well under production.

The dimensionless differential equation governing the unsteady radial flow was derived and presented in Chapter 4. It is:

$$\frac{\partial^2 p_D}{\partial r_D^2} + \frac{1}{r_D} \frac{\partial p_D}{\partial r_D} + \alpha \left( \frac{\partial p_D}{\partial r_D} \right)^2 = \frac{\partial p_D}{\partial t_D} \quad (6.1)$$

The initial and boundary conditions applicable to the situation where the well is under production (drawdown) are:

$$p_D(r_D, 0) = 0 \quad (6.2)$$

$$p_D(\infty, t_D) = 0 \quad (6.3)$$

$$\left. \frac{\partial p_D}{\partial r_D} \right|_{r_D=1} = -1 \quad (6.4)$$

The first boundary condition, Equation 6.2, states that pressure is equal to the initial pressure at all points prior to production. Equation 6.3 is

a statement of the fact that the flow is always transient; in other words, the system boundary is never encountered during the period of interest. Equation 6.4 is a specification of Darcy's law at the well.

Equation 6.1 is nonlinear with respect to  $p_D$ , and is linearized by making the following variable change suggested by Odeh and Babu (1987):

$$p_D = \frac{1}{\alpha} \ln u \quad (6.5)$$

Upon substitution of Eq. 6.5 into Eqs. 6.1 to 6.4, a new set of equations in terms of  $u$  results:

$$\frac{\partial^2 u}{\partial r_D^2} + \frac{1}{r_D} \frac{\partial u}{\partial r_D} = \frac{\partial u}{\partial t_D} \quad (6.6)$$

$$u(r_D, 0) = 1 \quad (6.7)$$

$$u(\infty, t_D) = 1 \quad (6.8)$$

$$\left. \frac{\partial u}{\partial r_D} \right|_{r_D=1} = -\alpha u \quad (6.9)$$

The method of Laplace transformation may be used to obtain a solution to the problem. Application of the Laplace transform to Eq. 6.6 and 6.7 gives:

$$\frac{d^2 \tilde{u}}{dr_D^2} + \frac{1}{r_D} \frac{d\tilde{u}}{dr_D} = s\tilde{u} - 1 \quad (6.10)$$

Equation 6.10 is the inhomogeneous modified Bessel equation of order zero, and has the general solution:

$$\tilde{u} = AI_0(\sqrt{sr_D}) + BK_0(\sqrt{sr_D}) + \frac{1}{s} \quad (6.11)$$

In Eq. 6.11,  $A$  and  $B$  are integration constants, and  $I_0$  and  $K_0$  are the modified Bessel functions of the first and second kinds respectively.

The Laplace transform of Eq. 6.8 is:

$$\tilde{u}(\infty, t_D) = \frac{1}{s} \quad (6.12)$$

As  $r_D$  tends to infinity, the  $K_0$  term in Eq. 6.11 tends to zero, whereas the function,  $I_0$ , tends to infinity. To satisfy the requirement of Eq. 6.12, the constant,  $A$ , must be equal to zero.

Thus:

$$\tilde{u} = BK_0(\sqrt{sr_D}) + \frac{1}{s} \quad (6.13)$$

The Laplace transform of the inner boundary condition, **Eq. 6.9**, is:

$$\left. \frac{d\tilde{u}}{dr_D} \right|_{r_D=1} = -\alpha\tilde{u} \quad (6.14)$$

An expression for  $B$  may be obtained by combining Eqs. 6.13 and 6.14.

This is:

$$B = \frac{\alpha}{s [\sqrt{s}K_1(\sqrt{s}) - \alpha K_0(\sqrt{s})]} \quad (6.15)$$

Thus the solution for  $u$  in Laplace space is:

$$\tilde{u} = \frac{\alpha K_0(\sqrt{sr_D})}{s [\sqrt{s}K_1(\sqrt{s}) - \alpha K_0(\sqrt{s})]} + \frac{1}{s} \quad (6.16)$$

Equation 6.16 is written in the alternative form:

$$\tilde{u} = \frac{\alpha K_0(\sqrt{sr_D})}{s} f(s) + \frac{1}{s} \quad (6.17)$$

where:

$$f(s) = \frac{1}{\sqrt{s}K_1(\sqrt{s}) - \alpha K_0(\sqrt{s})} \quad (6.18)$$

The inverse transform of  $1/s$  is 1, and the function,  $K_0(\sqrt{sr_D})/s$ , as the Laplace transform of the classic exponential-integral solution of the radial diffusivity equation.

For large times (small  $s$ ), the following approximation is appropriate [Churchill, 1944]:

$$K_1(\sqrt{s}) \approx \frac{1}{\sqrt{s}} \quad (6.19)$$

The approximation in Eq. 6.19 is equivalent to modelling the well as a line source.

When Eq. 6.19 is substituted into Eq. 6.18,  $f(s)$  is:

$$f(s) = \frac{1}{1 - \alpha K_0(\sqrt{s})} \quad (6.20)$$

For small values of  $a$ ,  $f(s)$  can be further approximated as a truncated binomial series, viz:

$$f(s) \approx 1 + \alpha K_0(\sqrt{s}) \quad (6.21)$$

The binomial expansion is valid for values for  $a$  and  $K_0(\sqrt{s})$  for which the following relation holds:

$$aK_0(\sqrt{s}) < 1 \quad (6.22)$$

Equation 6.22 implies the following inequality:

$$K_0(\sqrt{s}) < \frac{1}{a} \quad (6.23)$$

Dividing both sides of **Eq.** 6.23 by  $s$  (always positive), we get:

$$\frac{K_0(\sqrt{s})}{s} < \frac{1}{as} \quad (6.24)$$

with the inverse transform:

$$-\frac{1}{2}Ei\left(-\frac{1}{4t_D}\right) < \frac{1}{a} \quad (6.25)$$

The magnitude of  $a$  is of the order of 0.01. If we further approximate the  $Ei$  function by its logarithmic approximation, the inequality can be written as:

$$\frac{1}{2}[\ln t_D + 0.8] < 100 \quad (6.26)$$

This implies that  $t_D$  must satisfy the following approximate requirement:

$$t_D < e^{200} \quad (6.27)$$

For most practical situations this would be satisfied, and the binomial expansion should be valid.

The equation for  $\tilde{u}$  then becomes:

$$\tilde{u} = \frac{\alpha K_0(\sqrt{sr_D})}{s} [1 + \alpha K_0(\sqrt{s})] + \frac{1}{s} \quad (6.28)$$

$$= \frac{\alpha K_0(\sqrt{sr_D})}{s} + \alpha^2 \frac{K_0(\sqrt{s})K_0(\sqrt{sr_D})}{s} + \frac{1}{s} \quad (6.29)$$

To the first order in  $\alpha$ ,  $\tilde{u}$  is:

$$\tilde{u} = \frac{1}{s} + \frac{\alpha K_0(\sqrt{sr_D})}{s} \quad (6.30)$$

The inverse transform of **Eq. 6.30** is:

$$u = 1 - \frac{\alpha}{2} Ei \left( -\frac{r_D^2}{4t_D} \right) \quad (6.31)$$

The dimensionless pressure is given by:

$$\begin{aligned} p_D &= \frac{1}{\alpha} \ln u \\ &= \frac{1}{\alpha} \ln \left[ 1 - \frac{\alpha}{2} Ei \left( -\frac{r_D^2}{4t_D} \right) \right] \end{aligned} \quad (6.32)$$

At the wellbore,  $r_D = 1$ , and the wellbore pressure drop is:

$$p_{wD} = \frac{1}{\alpha} \ln \left[ 1 - \frac{\alpha}{2} Ei \left( -\frac{1}{4t_D} \right) \right] \quad (6.33)$$

Equation 6.33 was used to plot  $p_{wD}$  vs  $t_D$  on a semi-logarithmic graph for different values of  $\alpha$ , and is shown in Fig. 6.1. The figure also shows a plot using the exponential-integral solution derived on the basis of the linear theory ( $\alpha = 0$ ). The nonlinear result shows pressure drops that are less than those computed from the linear theory. This difference increases with time, indicating a dependency on drainage radius that was present in the steady and pseudo-steady cases. In drawdown tests, this difference is likely to be misinterpreted as a rate and time-dependent skin factor, although this

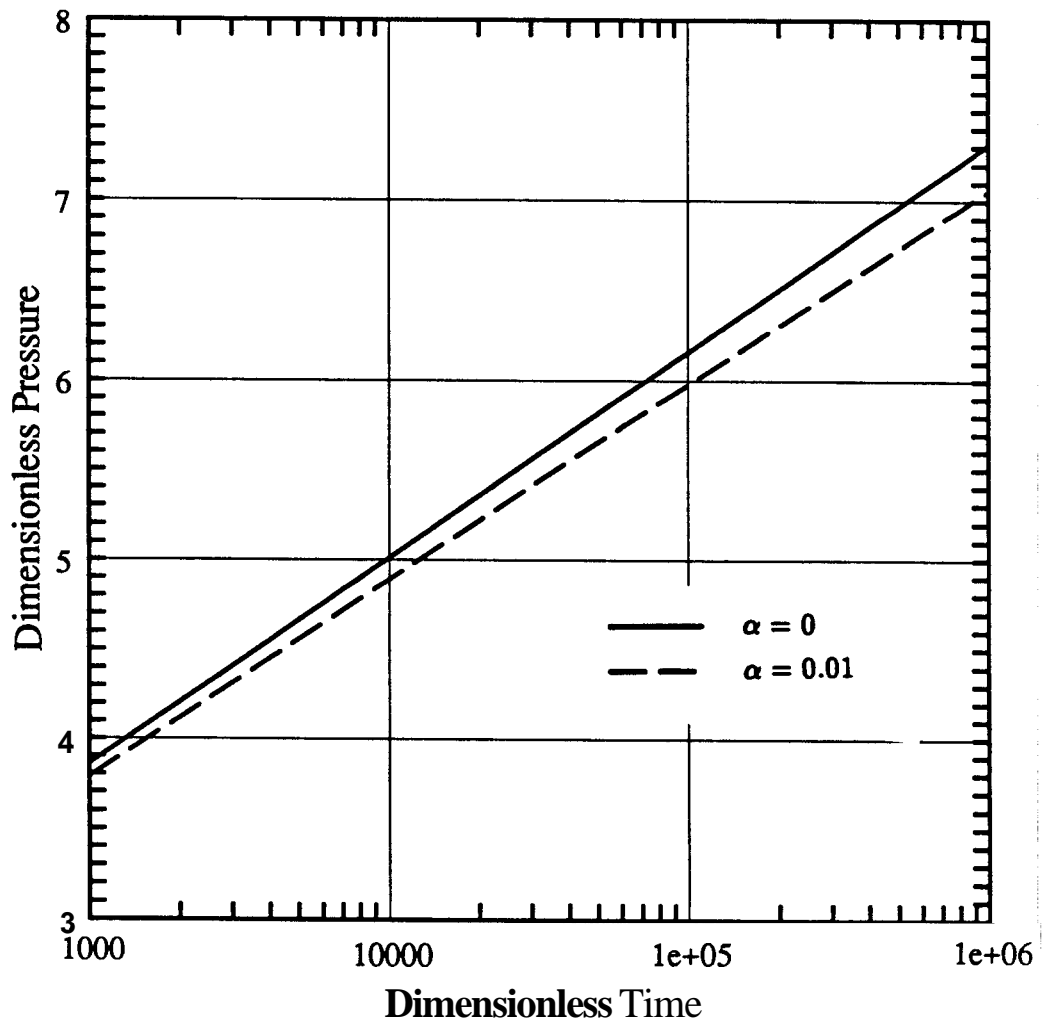


**Fig. 6.1** Drawdown Pressure Behavior

is merely an effect of the squared-gradient nonlinear term in the governing differential equation.

To further examine the nature of the pressure behavior, the logarithm term in Eq. 6.33 was expanded in a Taylor series. The expansion was to the first order in  $\alpha$ , and resulted in the following equation:

$$p_{wD} = -\frac{1}{2}Ei \left(-\frac{1}{4t_D}\right) - \frac{\alpha}{8}Ei^2 \left(-\frac{1}{4t_D}\right) \quad (6.34)$$

Equation 6.34 can be written in terms of dimensional pressures by recalling the definition of  $p_D$  :

$$p_i^2 - p_w^2 = Aq_{sc} - Bq_{sc}^2 \quad (6.35)$$

where the coefficients,  $A$  and  $B$  are given by:

$$A = -\frac{0.711(10^6)\mu zT}{kh} Ei \left(-\frac{1}{4t_D}\right) \quad (6.36)$$

$$B = \frac{0.253(10^{12})\mu zT^2b}{(kh)^2} Ei^2 \left(-\frac{1}{4t_D}\right) \quad (6.37)$$

## 6.2 Injection

The problem of a well injecting into an initially static reservoir will be discussed in this section. The governing equations for injection are identical to those for drawdown which were discussed in the previous section. The only difference is in the sign of the boundary condition at the well. The solution to the nonlinear injection problem is presented in this section.

The analysis starts off from Eq. 6.13 with the following equation for  $u$  in Laplace space:

$$\tilde{u} = BK_0(\sqrt{s}r_D) + \frac{1}{s} \quad (6.38)$$

The well boundary condition differs from that for drawdown only in sign, and is given by:

$$\left. \frac{d\tilde{u}}{dr_D} \right|_{r_D=1} = \alpha\tilde{u} \quad (6.39)$$

The integration constant,  $B$ , may be obtained by applying Eq. 6.39 to Eq. 6.38:

$$B = \frac{-a}{s[\sqrt{s}K_1(\sqrt{s}) + \alpha K_0(\sqrt{s})]} \quad (6.40)$$

Substituting Eq. 6.40 into Eq. 6.38, the solution is:

$$\tilde{u} = \frac{-\alpha K_0(\sqrt{s}r_D)}{s[\sqrt{s}K_1(\sqrt{s}) + \alpha K_0(\sqrt{s})]} + \frac{1}{s} \quad (6.41)$$

$$= \frac{-\alpha K_0(\sqrt{s}r_D)}{s} g(s) + \frac{1}{s} \quad (6.42)$$

where:

$$g(s) = \frac{1}{\sqrt{s}K_1(\sqrt{s}) + \alpha K_0(\sqrt{s})} \quad (6.43)$$

Equation 6.19 may be used to make an approximation of  $g(s)$ , valid for large times:

$$g(s) \approx \frac{1}{1 + \alpha K_0(\sqrt{s})} \quad (6.44)$$

which for small  $a$ , may be approximated by the binomial theorem as:

$$g(s) \approx 1 - \alpha K_0(\sqrt{s}) \quad (6.45)$$

Thus  $\tilde{u}$  is given by:

$$\tilde{u} = \frac{-\alpha K_0(\sqrt{sr_D})}{s} [1 - \alpha K_0(\sqrt{s})] + \frac{1}{s} \quad (6.46)$$

$$= \frac{-\alpha K_0(\sqrt{sr_D})}{s} - \alpha^2 \frac{K_0(\sqrt{s})}{s} K_0(\sqrt{sr_D}) + \frac{1}{s} \quad (6.47)$$

To the first order in  $\alpha$ , **Eq. 6.47** is:

$$\tilde{u} = -\frac{\alpha K_0(\sqrt{sr_D})}{s} + \frac{1}{s} \quad (6.48)$$

The inverse Laplace transform of **Eq. 6.48** is,

$$u = \frac{\alpha}{2} Ei\left(-\frac{r_D^2}{4t_D}\right) + 1 \quad (6.49)$$

The dimensionless pressure,  $p_D$ , is:

$$\begin{aligned} p_D &= \frac{1}{\alpha} \ln u \\ &= \frac{1}{\alpha} \ln \left[ 1 + \frac{\alpha}{2} Ei\left(-\frac{r_D^2}{4t_D}\right) \right] \end{aligned} \quad (6.50)$$

The pressure increase at the wellbore,  $p_{wD}$  may be obtained by replacing  $r_D$  by unity in **Eq. 6.50**. This results in:

$$p_{wD} = \frac{1}{\alpha} \ln \left[ 1 + \frac{\alpha}{2} Ei \left( -\frac{1}{4t_D} \right) \right] \quad (6.51)$$

The Taylor series expansion of  $p_{wD}$  to the first order in  $\alpha$  is:

$$p_{wD} = \frac{1}{2} Ei \left( -\frac{1}{4t_D} \right) - \frac{1}{4} \alpha Ei^2 \left( -\frac{1}{4t_D} \right) \quad (6.52)$$

Equation 6.52 suggests that the pressure increase computed by the nonlinear analysis is greater than that resulting from the linear theory, and that this difference increases with time. This observation is verified in Fig. 6.2, where  $p_{wD}$  is graphed against  $\ln t_D$  for both the linear and nonlinear cases.

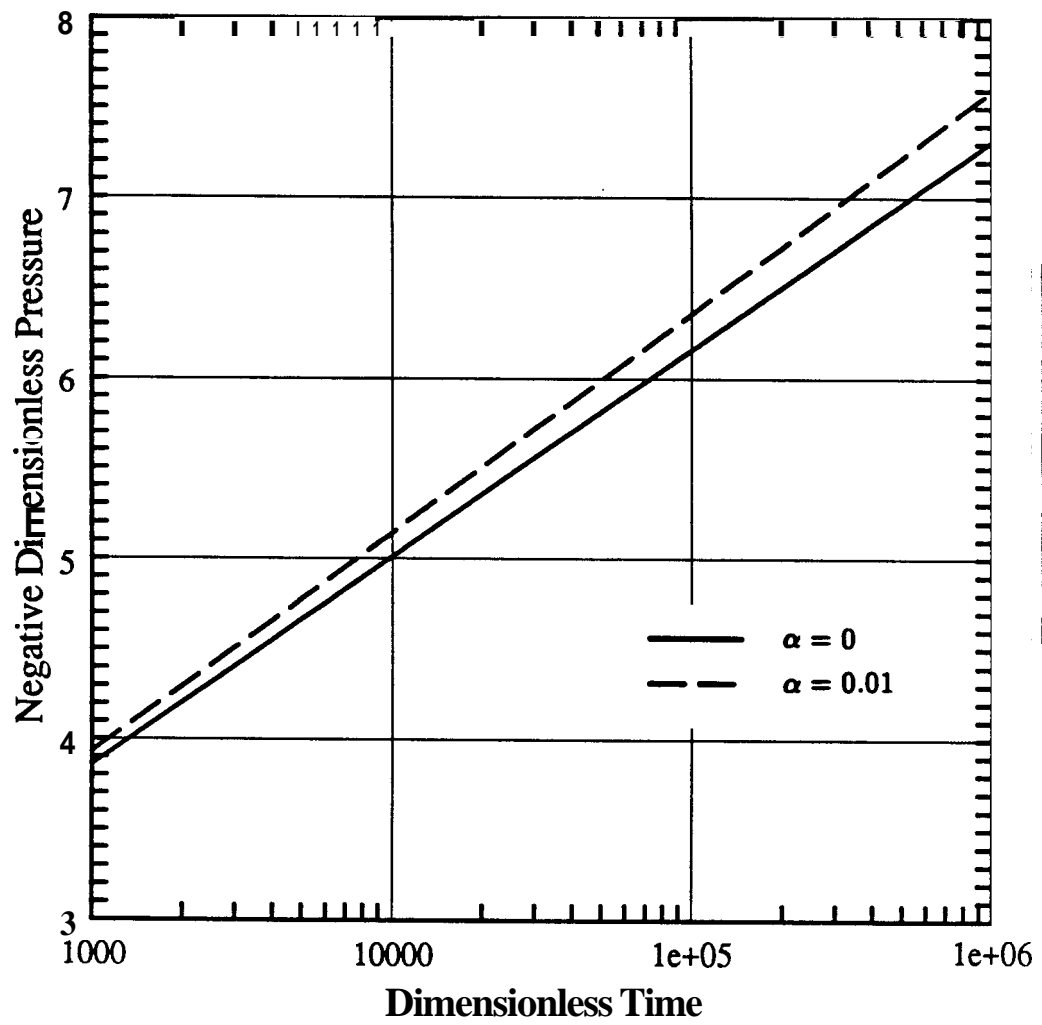


**Fig. 6.2 Injection Pressure Behavior**

# Chapter 7

## Conclusions

Several mathematical models have been developed to describe the nonlinear flow of gases in homogeneous porous media. The models were based on pressure and squared-pressure formulations and involved the integration of the fundamental equations governing the flow of gas in porous media. Darcy's law was assumed to be valid in all the analyses. Different kinds of geometries and flow regimes were considered. The objective of this study was to provide alternative analyses of the nonlinear pressure responses during gas flow through porous media. The following conclusions have been made on the basis of the results obtained in the study:

1. The analysis of steady flow through cores indicates that Darcy's law, in its differential form, is consistent with the finite form of the Forchheimer equation. Based on the excellent match of the equations with

experimental data, the observed deviations from linearity during high rate flow are more likely to be due to effects of real gas properties than to non-Darcy flow.

2. The onset of apparent non-Darcy flow can be predicted from a knowledge of a parameter,  $\alpha_1$ . Deviation from linearity occurs at an  $\alpha_1$  value of about 0.05, whereas the quadratic and cubic Forchheimer equations are applicable for  $\alpha_1$  values of up to **0.3** and 0.45 respectively. The parameter,  $\alpha_1$ , is proportional to Darcy velocity, viscosity, length and fluid compressibility, and inversely proportional to permeability.
3. The dimensionless time to ‘stabilization’ during unsteady flow through cores is the same, regardless of the magnitude of the pressure drop across the core. Steady state flow is reached at a dimensionless time,  $t_D$ , of about 0.4, and implies that stabilization will be slow for low permeability systems, long cores, high porosity rocks, and high fluid viscosity and compressibility.
4. Deviations from linearity during radial flow can be predicted on the basis of Darcian analyses.
5. Simulation of high rate gas wells requires the inclusion of nonlinear well terms to model the effects of drainage radius, and thus fluid property variations with pressure.

6. Darcy's law is applicable to a wider range of flow rates than has been previously thought.

## NOMENCLATURE

A	cross-sectional area
b	<b>gas</b> property parameter
C	gas performance coefficient
c	compressibility
h	formation thickness
K	hydraulic conductivity
k	permeability
L	length
M	molecular weight
n	<b>gas</b> performance index
P	pressure
q	volume flow rate
R	gas constant
r	radial distance
S	skin factor
s	Laplace transform parameter
T	temperature
t	time
v	velocity
x	linear distance
z	compressibility factor

$\alpha$	flow parameter
$\beta$	velocity coefficient
$E$	porosity
$\gamma_g$	gas specific gravity
$\mu$	viscosity
$\phi$	porosity

### Subscripts

c	critical
<b>D</b>	dimensionless
e	external boundary
g	gas
i	initial conditions
m	mean average
$\sigma$	equivalent length
sc	standard conditions
st	stabilization
t	total
w	wellbore

## Special Functions and Operators

$Ei$	exponential integral function
$I_0$	modified Bessel function of the first kind of order zero
$K_0$	modified Bessel function of the second kind of order zero
$L^{-1}$	inverse Laplace transform
$m(p)$	gas pseudo-pressure
$\mathbf{A}$	finite difference operator
$\mathbf{V}$	gradient operator

## REFERENCES

- Abou-Kassem, J. H. and K. Aziz:** “Analytical Well Models for Reservoir Simulation”, *Soc. Pet. Eng. J.*, (Aug. 1985) 573-579.
- Al-Hussainy, R.:** “Transient Flow of Ideal and Real Gases Through Porous Media”, Ph.D dissertation, Texas A & M University (1967).
- Al-Hussainy, R. and H. J. Ramey, Jr.:** “Application of Real Gas Flow Theory to Well Testing and Deliverability Forecasting”, *J. Pet. Tech.*, (May 1966) 637-642.
- Al-Hussainy, R., H. J. Ramey, Jr., and P. B. Crawford:** “The Flow of Real Gases Through Porous Media”, *J. Pet. Tech.*, (May 1966) 624-636.
- Aziz, K., L. Mattar, S. C. M. Ko, and G. S. Brar:** “Use of Pressure, Pressure-Squared or Pseudo-Pressure in the Analysis of Gas Well Data”, *J. Cdn. Pet. Tech.*, (April-June 1976) 58-65.
- Brigham, W. E.:** “Estimating Reservoir Parameters From the Gas Back-pressure Equation”, *SPEE*, (May, 1988) 649-650.
- Churchill, R. V.:**, *Operational Mathematics*, McGraw-Hill, New York (1944).
- Corbett, T. G. and R. A. Wattenbarger:** “An Analysis of the Cor-

rection for Gas Deliverability Curves”, paper SPE 14208, *presented at the 60th Annual Tech. Conf. and Exhib. of SPE*, Las Vegas, Nev., Sept. 22-25, 1985.

**Cornell, D.** : “ Flow of Gases Through Consolidated Porous Media ”, Ph.D dissertation, University of Michigan (1952).

**Cornell, D. and D. L. Katz:** “ Flow of Gases Through Consolidated Porous Media”, *Ind. and Eng. Chem.* (Oct. 1953) **45**, 2145.

**Craft, B. C. and M. F. Hawkins:** *Petroleum Reservoir Engineering*, Prentice-Hall, Inc., Englewood Cliffs, New Jersey (1959).

**Darcy, H.** : “ Les Fontaines Publiques de la Ville de Dijon ”, Dalmount, Paris (1856).

**Dranchuk, P. M. and L. J. Kolada:** “Interpretation of Steady Linear Visco-Inertial Gas Flow Data” *J. Cdn. Pet. Tech.*, (Jan-Mar 1968) 36-40.

**Dranchuk, P. M. and E. Chwyl:** “Transient Gas Flow Through Finite Linear Porous Media”, *J. Cdn. Pet. Tech.* (Apr-June 1969) 57-65.

**Dranchuk, P. M. and A. R. Piplapure:** “ Inertial and Slip Effects in Steady-State Radial Gas Flow Through Porous Media”, *J. Pet. Tech.* (Oct. 1973) 1155-1156.

**Dranchuk, P. M., R. A. Purvis and D. B. Robinson:** “ Computer Calculation of Natural Gas Compressibility Factors Using the Standing and Katz Correlations ”, *Inst. of Pet. Tech.*, IP-74-008 (1974).

**Elenbaas, J. R. and D. L. Katz:** “A Radial Turbulent Flow Formula”, *Trans., AIME*, (1948) **174**,25-40.

**ERCB :** *Theory and Practice of the Testing of Gas Wells*, Energy Resources Conservation Board. Calgary, Alberta (1975).

**Ezeudembah, A. and P. M. Dranchuk:** “Flow Mechanism of Forchheimer’s Cubic Equation in High-Velocity Radial Gas Flow Through Porous Media”, paper SPE 10979, *presented at the 57th Annual Tech. Conf. and Exhib. of SPE*, New Orleans, Louisiana, Sept. 26-29, 1982.

**Fancher, G. H. and J. A. Lewis:** “Some Physical Characteristics of Oil Sands”, *Ind. and Eng. Chem.* (1933) **25**, 1139.

**Finjord, J. and B. S. Aadony:** “ Effects of Nonlinear Gradient Term in Exact Analytical Solutions of the Radial Flow Equation for Oil in a Reservoir ”, *paper SPE 15069*, (1986) (under review).

**Finjord, J.:** “ Curling Up the Slope: Effects of the Quadratic Gradient Term in the Infinite-Acting Period for Two-Dimensional Reservoir Flow ”, *paper SPE 16451*, (1986) (under review)

**Firoozabadi, A. and D. L. Katz:** “ An Analysis of High-Velocity Gas Flow Through Porous Media”, *J. Pet. Tech.* (Feb. 1979), 211-216.

**Forchheimer, Ph.:** “Wasserbewegung durch Boden”, *Zeitz. ver. Deutsch Ing.* (1901) **45**, 1731.

**Geertsma, J:** “Estimating the Coefficient of Inertial Resistance in Fluid Flow Through Porous Media”, *Soc. Pet. Eng. J.* (Oct. 1974), 445-450.

**Gewers, C. W. W. and L. R. Nichol:** “Gas Turbulence Factors in a Microvugular Carbonate“, *J. Cdn. Pet. Tech.* (Apr-Jun 1969), 51-56.

**Green, L. and P. Duwez:** “Fluid Flow Through Porous Metals”, *J. Appl. Mech.* (Mar. 1951) **18**,39.

**Houpeurt, A.:** “On the Flow of Gases in Porous Media”, *Revue de L'Institut Français du Petrole*, (1959) **XIV** (11), 1468-1648.

**Hubbert, M. K.:** “Darcy’s Law and the Field Equations of Flow of Underground Fluids”, *Trans., AIME* (1956) **207**,222-239.

**Ikoku, C. U.:** *Natural Gas Reservoir Engineering* John Wiley and Sons, New York (1984).

**Jones, S. C.:** “ Using the Inertial Coefficient,  $\beta$ , to Characterize Heterogeneity in Reservoir Rock”, paper SPE 16949, presented at the 62nd Annual Tech. Conf. and Exhib., Sept. 27-30, 1987, Dallas, Tex.

**Kabir, C. S. and A. R. Hasan:** “ Prefacture Testing in Tight Gas Reservoirs ”, *SPEFE* (April 1986) 128-138.

**Kale, D. and L. Mattar:** “Solution of a Non-Linear Gas Flow Equation by the Perturbation Technique ”, *J. Cdn. Pet. Tech.* (Oct.-Dec. 1980) 63-67.

**Katz, D. L., D. Cornell, R. Kobayashi, F. H. Poettman, J. A. Vary, J. R. Elenbaas, and C. F. Weinaug:** *Handbook; of Natural Gas Engineering*, McGraw-Hill Book Co. Inc., New York City (1959).

**Klinkenberg, L. J. :** “ The Permeability of Porous Media to Liquids and Gases ”, *API Drilling and Production Practices*, pp 200-213 (1941).

**Lee, A. L., M. H. Gonzalez and B. E. Eakin :** “ The Viscosity of Natural Gases ”, *J. Pet. Tech.*, (Aug. 1966) 997-1000.

**Lee, J. :** *Well Testing;*, Soc. Pet. Engr. of AIME, Dallas (1982).

**Lee, R. L., R. W. Logan, and M. R. Tek:** “Effect of Turbulence on Transient Flow of Real Gas Through Porous Media”, *SPEFE*, (Mar. 1987) 108-120.

**Lin C. C. and L. A. Segel:**, *Mathematics Applied to Deterministic Problems in the Natural Sciences*, Macmillan, New York (1974).

**Muskat, M.:** *The Flow of Homogeneous Fluids Through Porous Media*", McGraw-Hill Book Co., Inc., New York (1937).

**Newberg, M. A. and H. Arastoopour:** "Analysis of the Flow of Gas Through Low-Permeability Porous Media", *SPE* (Nov. 1986) 647-653.

**Noman R. and J. S. Archer:** "The Effect of Pore Structure on Non-Darcy Gas Flow in Some Low Permeability Reservoir Rocks", paper SPE/DOE 16400, *presented at the SPE/DOE Low Permeability Reservoirs Symp.*, May 18-19, 1987, Denver, Colorado.

**Noman R., N. Shrimaker, and J. S. Archer:** "Estimation of the Coefficient of Inertial Resistance in High Rate Gas Wells", paper SPE 14207, *presented at the 60th Annual Tech. Conf. and Exhib. of SPE*, Sep 22-25, 1985, Las Vegas, Nevada.

**Odeh, A. S. and D. K. Babu:** "Comparison of Solutions of the Nonlinear and Linearized Diffusion Equation", *paper SPE 17270* (1987), under review.

**Peaceman, D. W.:** "Interpretation of Well-Block Pressures in Numerical Reservoir Simulation", *Soc. Pet. Eng. J.*, (June 1978) 183-194.

**Peaceman, D. W.:** "Interpretation of Well-Block Pressures in Numerical Simulation With Nonsquare Grid Blocks and Anisotropic Permeability", *Soc. Pet. Eng. J.* (June 1983) 531-543.

**Pedrosa, O. A. and K. Aziz:** “Use of Hybrid Grid in Reservoir Simulation”, *SPEERE* (Nov. 1986) 611-621.

**Ramey, H. J., Jr.:** “Non-Darcy Flow and Wellbore Storage Effects in Pressure Buildup and Drawdown of Gas Wells”, *Trans., AIME* (1966) **231**, 96.

**Ramey, H. J., Jr. and W. M. Cobb:** “A General Pressure Buildup Theory for a Well in a Closed Drainage Area”, *J. Pet. Tech.* (Dec. 1971) 1493-1505.

**Rawlins, E. L. and M. A. Schellhart:** *Back Pressure Data on Natural Gas Wells and their Application to Production Practices*, U.S. Bureau of Mines, Monograph 7 (1936).

**Rowan, G. and M. W. Clegg:** “An Approximate Method for Non-Darcy Radial Gas Flow”, *Soc. Pet. Eng. J.* (June 1964) 96-114.

**Russell, D. G., J. H. Goodrich, G. E. Perry, and J. F. Bruskotter:** “Methods for Predicting Gas Well Performance”, *J. Pet. Tech.* (Jan. 1966) 99-108.

**Swift, G. W. and O. G. Kiel:** “The Prediction of Gas-Well Performance Including the Effects of Non-Darcy Flow”, *J. Pet. Tech* (July 1962) 791-798.

**Tek, M. R. and K. H. Coats and D. L. Katz:** “The Effect of Turbulence on Flow of Natural Gas Through Porous Reservoirs”, *J. Pet. Tech.* (July 1962) 799-806.

**Tek, M. R., M. L. Grove, and F. H. Poettmann:** “Method of Predicting the Back Pressure Behavior of Low Permeability Natural Gas Wells”, *Trans., AIME* (1957) **210**, 302-309.

**Thomas, L. K., R. W. Hankinson, and K. A. Phillips,** “Determination of Acoustic Velocities for Natural Gas”, *J. Pet. Tech.* (July 1970) 889-895.

**Wattenbarger, R. A. and H. J. Ramey Jr.,:** “Gas Well Testing With Turbulence, Damage, and Wellbore Storage”, *J. Pet. Tech.* (May 1968) 877-887.

**Wycoff, R. D., H. G. Botset, M. Muskat, and D. W. Reed:** “Measurement of Permeability of Porous Media”, *Am. Assoc. Pet. Geol. Bulletin*, **18**(2), 161-190.